Name:
Date of Experiment:
Date of Report:
Date of Signature:
Signature:
Name of the Assistent:

F 17 Neutron Physics

Take this page as cover of your report please.

Abstract

The neutron was discovered by Chadwick in 1932. Since then the neutron has not only been of interest to fundamental physics but is also used as a tool to provide an insight into the solid state of matter as well as its dynamics. It has proved invaluable for today's scientific view of the world.

From the introduction of "Exploring matter with neutrons, Highlights in research at the ILL" [ILL00]:

Neutrons are subatomic particles found in the nuclei of atoms. They are emitted during certain nuclear processes including the fission of ^{235}U so can be obtained from a nuclear reactor. Like all subatomic particles neutrons obey the laws of quantum mechanics, which means they behave like waves as well as particles. The wavelength of neutrons (tens of nanometres) corresponds to the distances between atoms and molecules in solids and liquids. Consequently when they interact with matter for example, a regular array of atoms or molecules in a crystal lattice the neutron waves are reflected, or scattered. Waves reflected from similarly oriented planes of atoms in the crystal interfere and re-inforce each other periodically to produce a characteristic diffraction pattern (like water waves on a lake that meet after being reflected off two rocks). The pattern can be recorded as a series of peaks of the scattered neutron intensity, which provides information about the position of the atoms and the distance between them.

Neutrons scatter off hydrogen atoms quite strongly (unlike X-rays) so are also used to establish their positions in biological materials, particularly those containing water (H_2O). What is more, hydrogen scatters very differently from its heavier isotope, deuterium. This means that selected components in a structure can be highlighted by substituting hydrogen with deuterium. The degree of isotopic substitution can also be controlled such that the scattering strength in one part of a structure is the same as in the surrounding medium, rendering it invisible so that another part of the structure stands out in contrast.

As well as determining structure, neutron scattering also reveals the motions of atoms and molecules via an exchange of energy between the neutrons and the sample (inelastic scattering). Very small changes in energy measured at low temperatures may also be used to measure subtle quantum processes in exotic materials.

Neutrons also have a spin, or magnetic moment, which can interact with the electron spins in magnetic materials. Beams of polarised neutrons (in which all the spins are aligned) offer a unique tool for characterising exotic materials with complex magnetic structures an area of growing interest.

Another area of increasing importance, is the study of thin films and multilayers. Many of the most important biological, chemical and electronic/magnetic phenomena occur at surfaces and interfaces. Under appropriate experimental conditions, neutrons can be reflected off surfaces and interfaces so that the depth of the layers and their structure and dynamics can be determined.

Finally, the neutron itself is used to investigate the laws of Nature. ILL has facilities to prepare beams of neutrons of very low energies (cold neutrons) for extremely precise experiments on gravity and on particle properties significant in developing a unified theory of the fundamental particles and forces of the Universe.

In this lab, the knowledge of neutron physics was applied to exploit a neutron source for the purpose of several experiments. First, you will use the ^{3}*He counter tube* as an universal neutron detector and you will determine the the total cross section of different materials. Next, the neutron source will be used to activate unknown samples. The energy of the gamma radiation from these activated isotopes can be recorded by a Germanium detector and compared to theoretical decay schemes in order to identify the sources (*Activation Analysis*). Then, measuring the time of flight (*TOF*) spectrum of the neutron source you will learn a basic spectroscopic technique for beams of neutral particles. The neutrons are distributed with a typical moderator spectrum of a mean temperature to be determined. Finally, the *neutron camera* is another position sensitive neutron detector to make radiographies of any wanted probe.

To be successful, please be prepared **before** you come to the experiment. Important are the knowledge of interactions between neutron- and γ-radiation with matter (especially the absorption of neutrons and photoeffect, Compton-scattering and pair production of photons) as well as the different kinds of radioactive decays! The deconvolution of the TOF-measurement needs a small computer program, so **basics in programming languages** are needed; C would be perfect! Furthermore, you need some basic knowledge in solid state physics and high energy physics, **so the experiment should only be done in the second part of your Fortgeschrittenen-Praktikum!**

References:

- Krane, Kenneth S. Introductory Nuclear Physics. John Wiley & Sons
- W. R. Leo, Techniques for Particle Physics Experiments, Springer-Verlag, 1994 (chapter 1, 2.7, 2.8, 6 and 10.7)
- G. F. Knoll, Radiation Detection and Measurement, John Wiley & Sons, New York 1978 (chapter 1, 2, 12 and 14)
- P. R. Bevington, D. K. Robinson, Data Reduction and Error Analysis for the Physical Sciences, McGraw-Hill Inc., 1992 (chapter 4)

In parallel to your measurements, a structured and easily readable protocol has to be written including schemes of your setup, the parameters of your hardware and the most important values of your measurements.

The final report has to be self contained. Make sure that each part (measurement, data and error analysis) can be understood without further reference to the script. Please make sure that graphs and drawings are labeled properly and you make use of your word processor's spell checker.

The experiment takes place at 4 days a week (double experiment) at the **Physikalische Institut, Philosophenweg 12, in the cellar opposite to the elevator.**

Contents

Many thanks to Sarah Rice!

This english version of the script is based on her report.

If you will find errors in this script or if you will have any suggestions for improvement, please let the assistant know.

Chapter 1

Basics of Neutron Physics

1.1 The Neutron

Neutrons and protons are the building block of the nucleus of an atom. The neutron is made up of three quarks namely the (up, down, down) and thus is a Baryon. It has a relatively big mass, like the proton (m_n = 939.57 MeV/c^2, m_p = 938.28 MeV/c^2). Neutrons aren't stable outside the nucleus. They decay into a proton, electron and an electron-antineutrino (β-decay) with a mean life time of $\tau_n = 886.7 \pm 1.9$ seconds [Ca98]:

$$n \longrightarrow p + e^- + \bar{\nu_e} \ .$$

Neutrons are subject to all four fundamental interactions. Nuclear reactions and scattering at the nucleus potential are both strong interactions. The β-decay of a neutron is a weak interaction. Neutrons are uncharged particles and thus are unaffected by the Coulomb potential of the electrons. The electron magnetic interaction of the neutrons is only due to its spin coupling (spin-$\frac{1}{2}$) with the magnetic moment. The magnetic moment of neutrons is given by:

$$\mu_n = -1,91 \cdot \mu_K,$$

where

$$\mu_K = \frac{e \cdot \hbar}{2m_p} = 5.05 \cdot 10^{-27} \ \frac{J}{Tesla}$$

denotes the moment of one nucleon.

Neutrons can be divided into different groups depending on their kinetic energies:

- *Fast neutrons* have energy above 1 MeV and are usually produced in nuclear reactions. In this process, they gain kinetic energy as binding energy. The binding energy they carry is within 7-8 MeV per nucleon.
- *Epithermal neutrons* have energy between 0.4 eV and 1 MeV. They exist mainly in moderators produced by inelastic collisions on the moderator material.

- *Thermal neutrons* have very low energy of about 25 meV corresponding to a wavelength of 1.8 Å thus having a velocity of 2200 m/s. They are in thermal equilibrium with their moderator at room temperature, or about 300K, and so their energies are Maxwell distributed. Thermal neutrons are mostly used in solid state physics because the wavelength is in order of lattice constant and hence high resolution is obtained.
- *Slow or Cold neutrons* have energies of about 2 meV and are in thermal equilibrium with a very cold environment e.g. liquid Deuterium (about 25 K). Furthermore there exist *very cold* ($0.3\ \mu eV \leq E_n < 50\ \mu eV$) and *ultracold* ($E_n < 300\ neV$) neutrons [By94].

According to their kinetic energy or velocity neutrons can be described by their de Broglie wavelength:

$$\lambda = \frac{h}{m_n \cdot v}\ . \tag{1.1}$$

1.2 Interaction with matter

Since neutrons are electrically neutral, they can interact with the coulomb barrier only with their magnetic moment. Hence the dominant interaction is only with the nucleus of atoms in a material, not the electrons. The dominant processes are scattering and absorption. To describe these processes, the concept of cross section is used. The *cross section*, σ, is a measure of the probability that a particle interacts with another particle. It has the dimension of area. The main unit is the barn (1 barn = 10^{-24} cm^2):

$$\sigma = \frac{number\ of\ scattering\ prosesses\ per\ time}{incident\ particle\ density}\ .$$

The total cross section, σ_{tot}, is given as:

$$\sigma_{tot} = \sigma_{scatt} + \sigma_{abs},$$

where σ_{scatt} denotes the scattering cross section and σ_{abs} the absorption cross section.

The scattering can be elastic or inelastic, as well as coherent or incoherent:

$$\sigma_{scatt} = \sigma_{elast} + \sigma_{inelast} \quad or \quad \sigma_{scatt} = \sigma_{coh} + \sigma_{inc}.$$

During *elastic scattering* (n, n), the nucleus carries only momentum. During *inelastic scattering* (n, n'), part of the kinetic energy of the neutrons is lost. *Coherent scattering* is when the entire scattered wave from the probe has the same phase relation, so that constructive interference in the form of Bragg-Peaks occurs. *Incoherent scattering* is due to the different nuclear spin orientation and different isotopes of the material.

Absorption is due to the following reactions:

$$\sigma_{abs} = \sigma(n,\gamma) + \sigma(n,\alpha) + \sigma(n,\beta) + \sigma(n,p) + \sigma(n,fission).$$

The absorption cross section as well as the incoherent cross section depends strongly on the neutrons' energy:

$$\sigma_{abs,inc} \sim t \sim \frac{1}{v} \implies \sigma_{abs,inc}(v) = \sigma_0 \cdot \frac{v_0}{v} \ . \tag{1.2}$$

The cross sections decrease with an increase in the neutrons' velocity. Thus, as neutrons slow down (become moderated) due to inelastic scattering processes, the absorption cross section increases, and interactions become more probable.

The weakening of a monoenergetic neutron flow, φ, through a material of thickness x is given by:

$$d\varphi = \sigma_{tot} \cdot n_B \cdot \varphi \cdot dx, \tag{1.3}$$

where σ_{tot} denotes the *total cross section* and $n_B = N_A \cdot \frac{\rho}{A}$ the particle density.

$$\Sigma_{tot} = \sigma_{tot} \cdot n_B \tag{1.4}$$

Σ_{tot} is called the *macroscopic cross section*. Σ_{tot} is the inverse of the *mean free path* l:

$$\varphi(x) = \varphi_0 \cdot e^{-\Sigma_{tot} \cdot x} = \varphi_0 \cdot e^{-\frac{x}{l}} \ . \tag{1.5}$$

1.3 Neutron Sources

Beams of neutrons can be produced form a variety of nuclear reactions.

- It is the oldest method which involves the firing of Beryllium atoms with alpha radiations. Examples of alpha emitters used are Polonium, Radium or Americium. The neutrons emitted aren't monoenergetic.

- *Spallation sources*: A proton radiation of high energy is enclosed in a Tungsten target. It builds a highly stimulated compound nucleus. As the compound nucleus lost energy, it produces neutrons. There are a few sources of this modern concept in planning or construction around the world (see e.g. the European Spallation Source "ESS": www.kfa-juelich.de/ess/).

- *Stimulated fission*: It is one of the most effective neutron sources. Here the nucleus absorbs neutrons and undergo nuclear fission. Thus neutrons are emitted. There exist a lot of specialized research reactors as at the Institut Laue-Langevin (ILL) in Grenoble (www.ill.fr and [Ye97]).

- *Spontaneous Fission*: A common source of neutrons is the spontaneous fission of isotopes such as ^{252}Cf. The neutron energies are continuous.

1.4 The experimental neutron source ^{252}Cf

Production and properties of ^{252}Cf

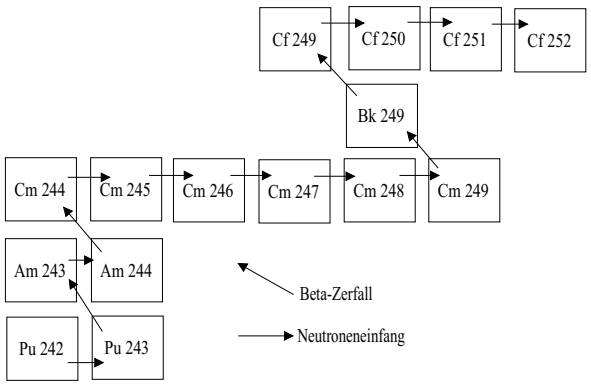

Figure 1.1: Production of ^{252}Cf in a series of 14 nuclear reactions, starting at ^{242}Pu or ^{243}Am.

In this experiment, the neutrons were produced from ^{252}Cf which has a half life of 2.63 years, where 97% of its reaction is by β-decay and 3% by spontaneous fission. 20 μg of ^{252}Cf was used for the source in the experimental setup; when it decays, it produces $4.68 \cdot 10^7$ neutrons per second (status of summer 1998 [Ma98]).

Setup of the neutron source

In the experimental source, the neutrons are emitted in every direction and at higher velocities than thermal. In order to control their direction and decrease their velocity, the source is placed in a housing that is made up of layers of various materials (see fig. 1.2):

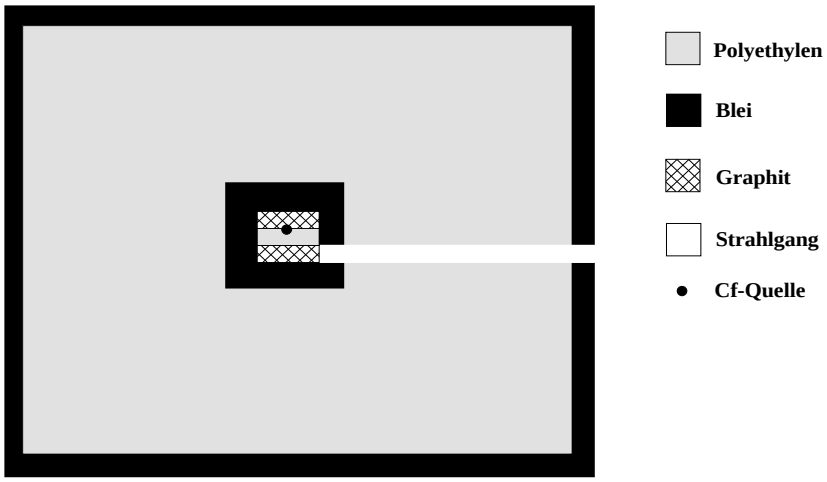

Figure 1.2: Setup and shielding of the neutron source.

- Polyethylene is used as a moderator because it is cheap and it doesn't need to be cooled.
- Lead is used because it absorbs the gamma rays produced when neutrons are absorbed and binding energy is released. Thus, it acts as a biological shield.

- Graphite is used to direct neutrons because of its high cross section, which makes it a strong scattering material which absorbs few neutrons [Ma98].

Up to the surface of the polyethylene block almost all neutrons were absorbed, but there was still much gamma rays emitted. Thus, more lead shield of about 10 cm was used for biological shielding.

Because thermal neutrons were needed, the emitted neutrons, with average energy of 2.14 MeV, produced from this Californium source were moderated. Polyethylene was used as the moderator because it is rich in hydrogen, which has a large inelastic and incoherent scattering cross section, and has about the same mass as a neutron. Hence, the neutrons lose much of their kinetic energy before exiting the housing.

Chapter 2

Detecting Neutrons

Most detectors operate based on the ionisation capacity of charged particles as they pass through its active material. Neutrons, which are uncharged, can't be detected in this way; the information the neutrons carry has to be converted to charged particles through a nuclear reaction. In this experiment, a ^{3}He-detector is used to determine the pulse height spectrum.

2.1 The ^{3}He-Detector

The ^{3}He-detector consists of a metal tube filled with gaseous ^{3}He. A thin wire in the middle of the tube is used as an anode for a high voltage. The geometry of the counter tube is the typical geometry of a Geiger-Müller counter tube. In the ^{3}He-detector, the neutrons are converted to a tritium nucleus and a proton according to the (n, p)-nuclear reaction:

$$^3He + n \longrightarrow {}^3H + p + 764\ keV.$$

The cross section of the above reaction using thermal neutrons is 5327 barn. Using a high filling pressure of 8 bar a high detection efficiency of nearly 95% can be reached. The reaction energy, Q, is shared between the particles as follows: $\frac{1}{4}$Q = 191 keV for the tritium and $\frac{3}{4}$Q = 573 keV for the proton. These charged particles ionize the gas molecules in the detector as they move through it. Thus, the ^{3}He-gas isn't only a neutron converter, but also a counting gas.

The resulting electron/ion pairs are accelerated towards the anode and the cathode, respectively, by the gradient of the electric field. Close to the anode the electrons are accelerated sufficiently to cause gas amplification by ionisation of further gas atoms.

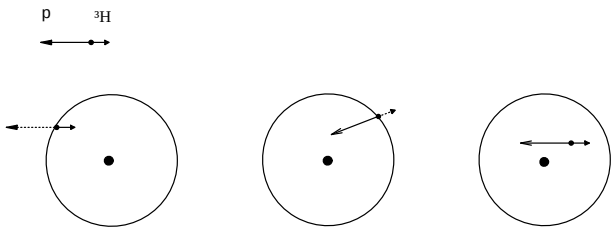

Figure 2.1: Schematic: cross section of a ^{3}He counter tube. Possible ionisation tracks within the detector tube.

Those particles produced beside the detector's wall, would not deposit their entire energy in the gas volume in case of collision with the wall. This gives rise to "wall effects" in the pulse height spectrum (see fig. 2.2), which depends solely on the geometric construction of the detector.

One can clearly see the edge in the count rate at 191 keV. Here only the tritium has deposited its energy in the gas. At 573 keV there is another edge. Here the proton has deposited completely its energy. At 764 keV both particles have given up their hole energy by ionisation. Counts far above 764 keV result of several counted neutrons at the same time (so called *Pile-Up's*).

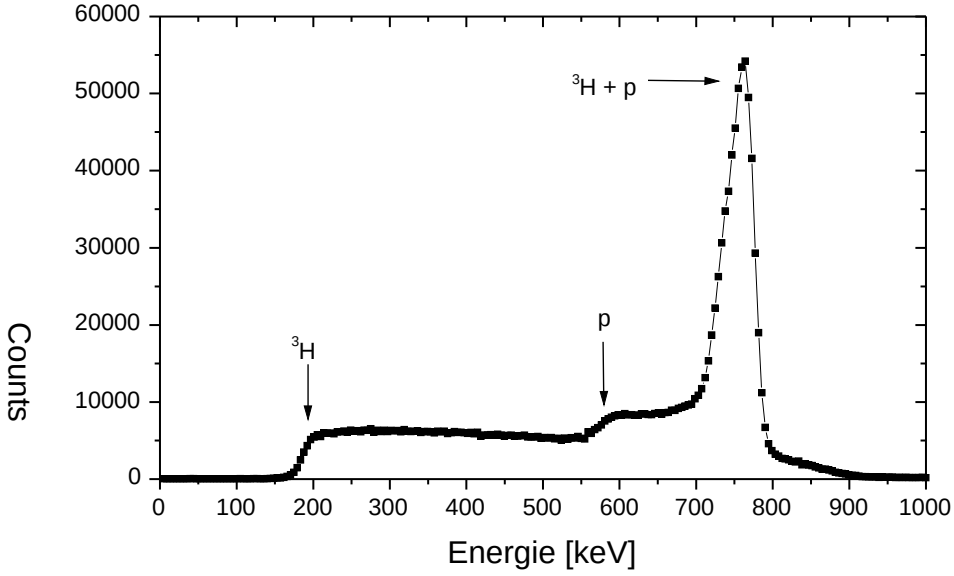

Figure 2.2: Measured pulse height spectrum of a ^{3}He-detector.

2.2 Measurements

Setup

The schematic setup of the electronic used to convert a signal from the detector into data to be imputed into an ADC in a CAMAC crate is as follows (see figure 2.3):

At first, a high voltage of about +1000 V is applied to the detector. The detector signal then is guided to the preamplifier via one capacity to protect the preamp of the high voltage. The preamplifier itself is used to convert the charge pulse from the detector into a voltage signal. The main amplifier provides the voltage gain to increase the negative milli-volt preamp signal (about -200 mV) to a range of a few volts of positive polarity (0-4 V), where it can be more conveniently processed. The main amplifier must be linear, so that the proportionality of the radiation energy and the pulse height can be preserved.

One of the Peak-ADC's (ADC = Analog to Digital Converter) in the CAMAC crate is used to display the many pulse heights that are produced by the nuclear reaction, with the pulse height on the horizontal scale and the number of pulses on the vertical. The input pulses are digitalised, and the digital pulse height is stored in a memory location referred to as channel. The resulting pulse height spectrum (see fig. 2.2) can then be used to determine the energies of the radiations, in our case tritium and proton.

The discriminator is used to set the threshold level, which determines the minimum height of the signal to be seen; if the threshold is too low, too much noise will be included in the data. If it is

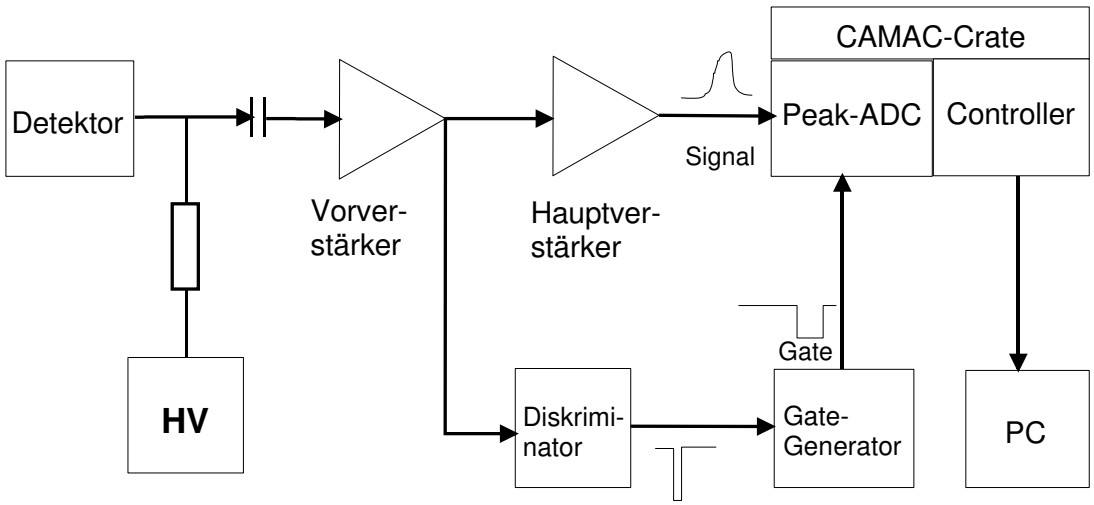

Figure 2.3: Setup of the detector readout electronic.

too high, some of the data could be lost. The signal of the discriminator starts a gate generator. The gate generator produces then a norm pulse of desired polarity and selected length in time. Using this gate signal the Peak-ADC knows the time interval to search for a peak and to convert him. The Peak-ADC needs a negative norm pulse on its 'Gate'-input.

- The signals at every point in the setup should be observed on the oscilloscope and **should be** protocolled with a small plot (**named axis inclusive**)!

Measurement of the pulse height spectrum

- The pulse height spectrum (PHS) has to be taken twice, each time for 600 s, once with the lowest possible and once with the optimal threshold. The PHS with the lowest threshold has a lot of noise due to external environment, but a few neutrons were still detected. The threshold has to be increased until no gamma rays are detected and only neutrons could be seen. This can be checked using a sheet of Bor-plastic; since it absorbs neutrons, the sheet is placed between the source and the detector, and there should be no signal, since the threshold level removes the gamma rays and the Bor-plastics prevents the neutrons from being detected.
- The PHS with optimal threshold has very little noise. The relative positions of the energies of tritium and proton have to be checked.

Measurement of the total cross section

- To determine the total cross section σ_{tot} of different materials (see table 2.1), a PHS is first to be taken without any probe, and the detector at a specific position, for 600 s. Then, various probes are placed in front the neutron beam, with the detector at the same position, and their respective PHS taken. Since neutrons are emitted randomly, their distribution of their concentration in the atmosphere differs. Thus the position of the detector should

be fixed to avoid changing the reference signal derived from the beam. From the ratio of counts with and without any probe one can determine the total cross section σ_{tot} according to equation (1.5) and (1.4). **Don't** forget the calculation of the error bars!

Element	Density [g/cm^3]	Atom Mass [g/mol]	σ_{coh} [barn]	σ_{inc} [barn]	σ_{abs} [barn]
Aluminium	2.7	26.98	1.495	0.008	0.231
Lead	11.34	207.2	11.115	0.003	0.171
Nickel	8.91	58.71	13.3	5.2	4.49
Hydrogen			1.76	80.26	0.33
(Cadmium)	8.65	112.4	3.04	3.46	2526.5

Table 2.1: Data of the probes for the transmission measurements; given are the values for thermal neutrons (v_0 = 2200 m/s).

Please pay attention to following points: Regarding the actual neutron source (see figure 1.2), it is clear that no monochromatic neutron beam is here available. As you will see in the time of flight (TOF) measurement in chapter (4), the neutron spectrum is a very broad Maxwell spectrum with background of epithermal neutrons. This constant underground can be determined independently by measuring the neutron flux through a cadmium sheet. The cross section of cadmium in figure (2.4) shows, that cadmium is opaque for thermal neutrons, but for epithermal neutrons it is transparent. For this reason, cadmium is often used in neutron physics to determine the ratio between thermal and epithermal neutrons in a beam.

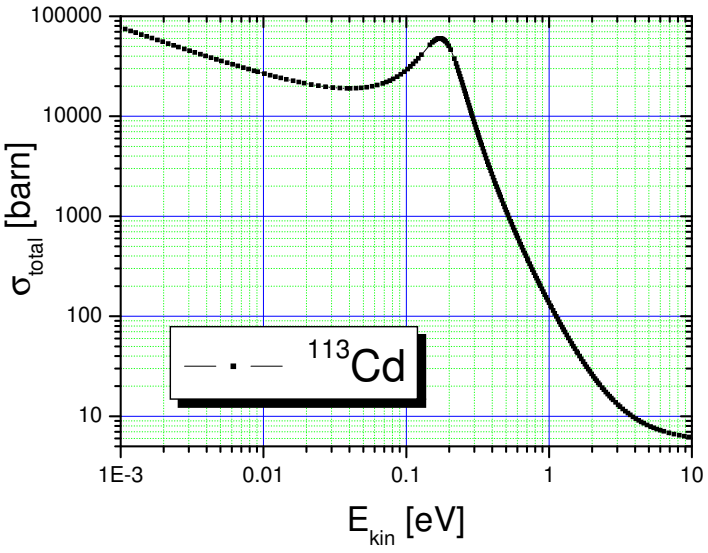

Figure 2.4: Behavior of the total cross section of ^{113}Cd depending of the kinetic energy of the neutron. ^{113}Cd is part of natural cadmium with 12% and it is responsible of the high absorption of thermal neutrons.

By measuring the transmission through cadmium the background of epithermal neutrons can be determined!

As preparation, calculate the transmission of thermal neutrons through 1 mm cadmium according to equation (1.5).

Furthermore, it is important to remember on to the mean velocity v of the neutron beam. v will be determined by the measurement of the time of flight distribution in chapter (4)! The real theoretic total cross section can be calculated according to equation (1.2) of the ratio between v_0 and v!

Chapter 3

Activation Analysis

This method is used to determine an unknown composition of isotopes in a material. In this experiment, three probes from eleven possible samples, will be analyzed using a Germanium-detector. This is a semiconductor detector. The probes were activated overnight inside the neutron source. When taken out of the neutron source, they under go β-decay and mostly gamma rays are emitted, which are detected by the Ge-detector. The pulse height spectra (PHS) obtained from the different probes can then used to identify the probes. This will be done by identifying the most prominent peaks in the spectrum, and then comparing the obtained value with a group of given theoretical decay schemes in the appendix.

The following introduction into semiconductor detectors has been taken from "W. R. Leo, Techniques for Particle Physics Experiments, Springer-Verlag, 1994".

3.1 The Germanium-Detector

Semiconductor detectors, as their name implies, are based on crystalline semiconductor materials, most notably silicon and germanium. These detectors are also referred to as solid-state detectors. The basic operating principle of semiconductor detectors is analogous to gas ionisation devices. Instead of a gas, however, the medium is now a solid semiconductor material. The passage of ionizing radiation creates electron-hole pairs (instead of electron-ion pairs) which are then collected by an electric field. The advantage of the semiconductor, however, is that the average energy required to create an electron-hole pair is some 10 times smaller than that required for gas ionisation. Thus the amount of ionisation produced for a given energy is an order of magnitude greater resulting in increased energy resolution. Moreover, because of their greater density, they have a greater stopping power than gas detectors. They are compact in size and can have very fast response times. Except for silicon, however, semiconductors generally require cooling to low temperatures before they can be operated. This, of course, implies an additional cryogenic system which adds to detector overhead.

3.1.1 Energy band structure of solids

Semiconductors are crystalline materials whose outer shell atomic levels exhibit an energy band structure. Figure (3.1) schematically illustrates this basic structure consisting of a valence band, a "forbidden" energy gap and a conduction band.

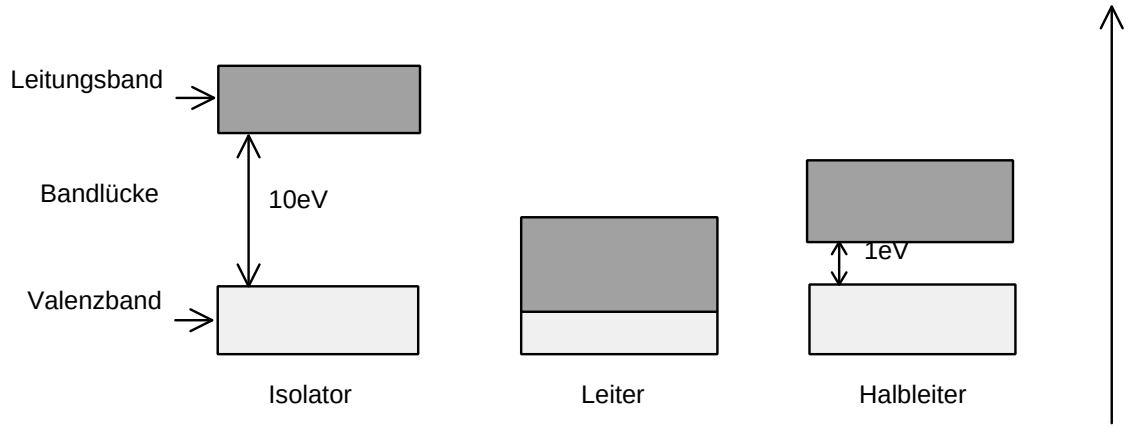

Figure 3.1: The band configuration for insulators, conductors and semiconductors are shown for comparison.

The energy bands are actually regions of many discrete levels which are so closely spaced that they may be considered as a continuum, while the "forbidden" energy gap is a region in which there are no available energy levels at all. This band structure arises because of the close, periodic arrangement of the atoms in the crystal which causes an overlapping of the electron wavefunctions. Since the Pauli-principle forbids more than one electron in the same state, the degeneracy in the outer atomic shell energy levels breaks to form many discrete levels only slightly separated from each other. As two electrons of opposite spin may reside in the same level, there are as many levels as there are pairs of electrons in the crystal. This degeneracy breaking does not affect the inner atomic levels, however, which are more tightly bound.

The highest energy band is the conduction band. Electrons in this region are detached from their parent atoms and are free to roam about the entire crystal. The electrons in the valence band levels, however, are more tightly bound and remain associated to their respective lattice atoms. The width of the gap and bands is determined by the lattice spacing between the atoms. These parameters are thus dependent on the temperature and the pressure. In conductors, the energy gap is nonexistent, while in insulators the gap is large. At normal temperatures, the electrons in an insulator are normally all in the valence band, thermal energy being insufficient to excite electrons across this gap.

In a semiconductor, the energy gap is intermediate in size such that only a few electrons are excited into the conduction band by thermal energy. When an electric field is applied, therefore, only a small current is observed. If the semiconductor is cooled, however, almost all the electrons will fall into the valence band and the conductivity of the semiconductor will decrease.

3.1.2 The np-junction

In a pure semiconductor crystal, the number of holes equals the number of electrons in the conduction band. This balance can be changed by introducing a small amount of impurity atoms having one more or one less valence electron in their outer atomic shell. For silicon and germanium which are tetravalent, this means either pentavalent atoms or trivalent atoms. These impurities integrate themselves into the crystal lattice to create what are called doped or extrinsic semiconductors. If the dopant is pentavalent, the situation in figures (3.2) and (3.3) arises. In

the ground state, the electrons fill up the valence band which contains just enough room for four valence electrons per atom.

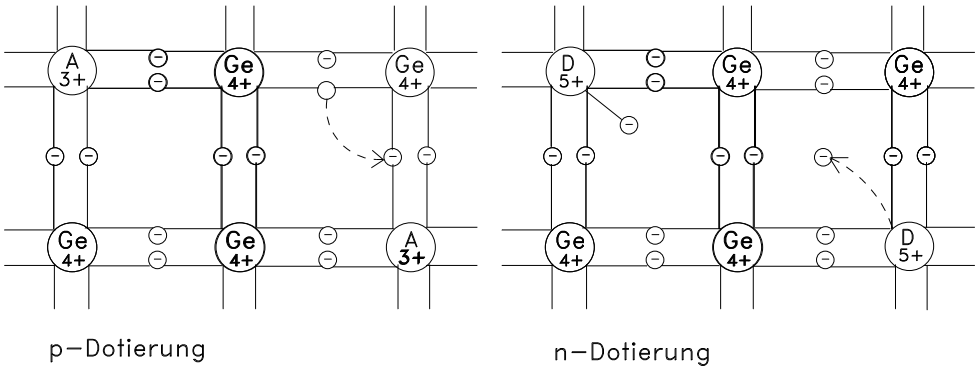

Figure 3.2: Addition of donor impurities to form n-type semiconductor materials. The impurities add excess electrons to the crystal and create donor impurity levels in the energy gap. In practice, donor elements such as arsenic, phosphorous and antimony are used to make n-type semiconductors, while gallium, boron and indium are most often employed as acceptor impurities for p-type materials.

Since the impurity atom has five valence electrons, an extra electron is left which does not fit into this band. This electron resides in a discrete energy level created in the energy gap by the presence of the impurity atoms.

Unlike recombination and trapping states, this level is extremely close to the conduction band being separated by only 0.01 eV in germanium and 0.05 eV in silicon. At normal temperatures, therefore, the extra electron is easily excited into the conduction band where it will enhance the conductivity of the semiconductor. In addition, the extra electrons will also fill up holes which normally form, thereby decreasing the normal hole concentration. In such materials, then, the current is mainly due to the movement of electrons. Holes, of course, still contribute to the current but only as minority carriers. Doped semiconductors in which electrons are the majority charge carriers are called n-type semiconductors.

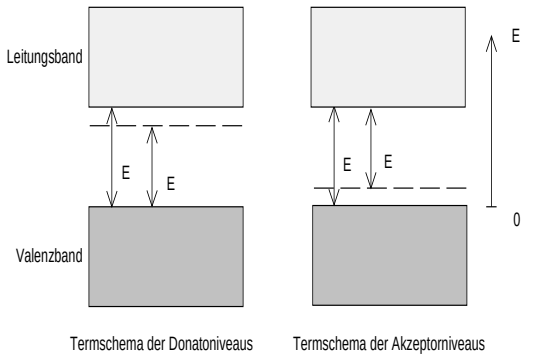

Figure 3.3: Addition of acceptor impurities to create p-type material. Acceptor impurities create an excess of holes and impurity levels close to the valence band.

If the impurity is now trivalent with one less valence electron, there will not be enough electrons to fill the valence band. There is thus an excess of holes in the crystal (figures 3.2 and 3.3). The trivalent impurities also perturb the band structure by creating an additional state in the energy gap, but this time, close to the valence band as shown in figure (3.3). Electrons in the valence band are then easily excited into this extra level, leaving extra holes behind. This excess of holes also decreases the normal concentration of free electrons, so that the holes become the majority charge carriers and the electrons minority carriers. Such materials are referred to as p-type semiconductors.

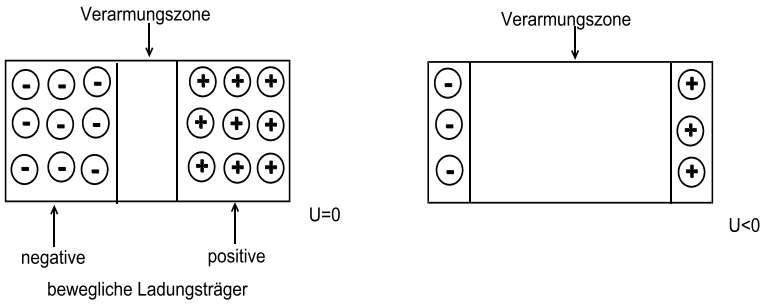

Figure 3.4: Schematic diagramm of an np junction.

The formation of a pn-junction creates now a special zone about the interface between the two materials. This is illustrated in figure (3.4). Because of the difference in the concentration of electrons and holes between the two materials, there is an initial diffusion of holes towards the n-region and a similar diffusion of electrons towards the p-region. As a consequence, the diffusing electrons fill up holes in the p-region while the diffusing n-holes capture electrons on the n-side. Recalling that the n and p structures are initially neutral, this recombination of electrons and holes also causes a charge build-up to occur on either side of the junction. Since the p-region is injected with extra electrons it thus becomes negative while the n-region becomes positive. This creates an electric field gradient across the junction which eventually halts the diffusion process leaving a region of immobile space charge. Because of the electric field, there is a potential difference across the junction. This is known as the contact potential.

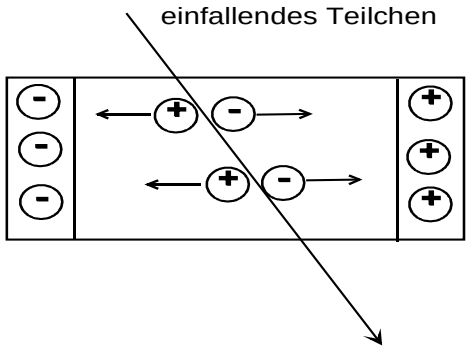

Figure 3.5: Production of electron-ion-pairs in a germanium crystal along the track of on ionising particle.

The region of changing potential is known as the depletion zone or space charge region and has the special property of being devoid of all mobile charge carriers. And, in fact, any electron or hole created or entering into this zone will be swept out by the electric field. This characteristic of the depletion zone is particularly attractive for radiation detection. Ionising radiation entering this zone will liberate electron-hole pairs which are then swept out by the electric field. If electrical contacts are placed on either end of the junction device, a current signal proportional to the ionisation will then be detected. The analogy to an ionisation chamber thus becomes apparent (see figure 3.5).

While the pn-junction described above will work as a detector, it does not present the best operating characteristics. In general, the intrinsic electric field will not be intense enough to provide efficient charge collection and the thickness of the depletion zone will be sufficient for stopping only the lowest energy particles. As we will see later, this small thickness also presents a large capacitance to the electronics and increases noise in the signal output. Better results can be obtained by applying a reverse-bias voltage to the junction, i.e., a negative voltage to the p-side, as shown in figure (3.4). This voltage will have the effect of attracting the holes in the p-region away from the junction and towards the p contact and similarly for the electrons in the n-region.

The net effect is to enlarge the depletion zone and thus the sensitive volume for radiation detection; the higher the external voltage, the wider the depletion zone. Moreover, the higher external voltage will also provide a more efficient charge collection.

3.1.3 The detector signal

The behavior of photons in matter (in our case, X-rays and γ-rays) is dramatically different from that of charged particles. In particular, the photon's lack of an electric charge makes impossible the many inelastic collisions with atomic electrons so characteristic of charged particles. Instead, the main interactions of X-rays and γ-rays in matter are photoeffect, Compton scattering and pair production (see figure 3.6).

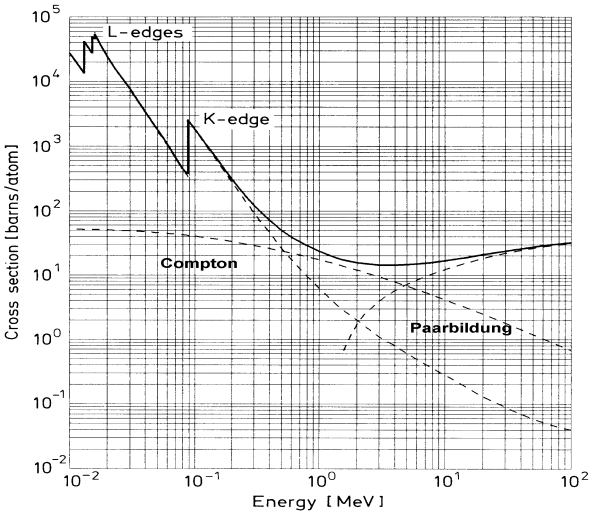

Figure 3.6: Photon cross sections for lead.

All 3 processes are shown in figure (3.7). The photoelectric effect involves the absorption of a photon by an atomic electron with the subsequent ejection of the electron from the atom. Compton scattering is the scattering of photons on free electrons. In matter, of course, the electrons are bound; however, if the photon energy is high with respect to the binding energy, this latter energy can be ignored and the electrons can be considered as essentially free. The process of pair production involves the transformation of a photon into an electron-positron pair. In order to conserve momentum, this can only occur in the presence of a third body, usually a nucleus. Moreover, to create the pair, the photon must have at least an energy of 1.022 MeV.

These reactions explain the two principal qualitative features of X-rays and γ-rays: (1) X-rays and γ-rays are many times more penetrating in matter than charged particles, and (2) a beam of photons is not degraded in energy as it passes through a thickness of matter, only attenuated in intensity.

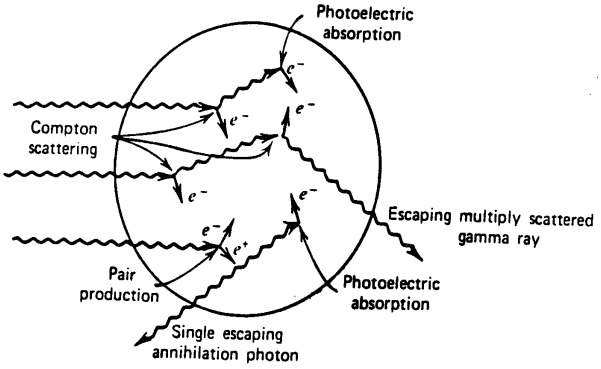

Figure 3.7: Schematic of the possible processes at the absorption of γ-rays in the detector crystal [Kr88].

Figure (3.8) shows the typical detector response for a monoenergetic γ-ray. There is the photopeak, where the hole energy of the γ-quantum was absorbed within the detector. Furthermore one can see the Compton continuum of the electrons produced by Compton scattering. If one or even both photons from the pair production event can escape out of the detector (see

figure 3.7), so a signal will be produced with energy of the photopeak reduced of the restmass ($m_e = 511$ keV/c^2) of one (*Single*) or two electrons (*Double escape peak*).

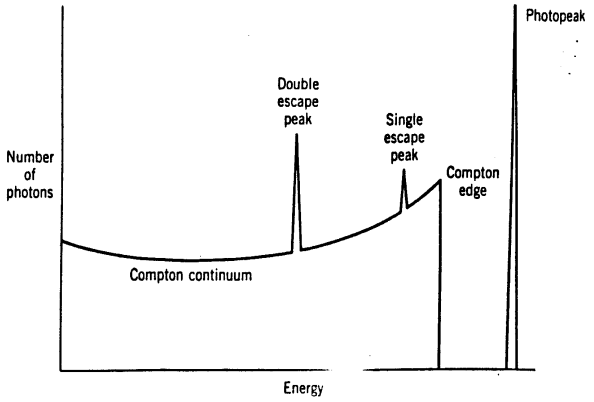

Figure 3.8: Typical spectrum of a monoenergetic γ-ray.

All these processes will produce free electrons in the germanium crystal, which will result in electron-hole-pairs. The applied voltage will guide all electrons to the anode, so that we get a pulse which can be read out by a preamplifier. The number n of produced electron-hole-pairs is proportional to the amount of absorbed energy E_γ of the γ-ray:

$$n = \frac{E_\gamma}{\epsilon}, \tag{3.1}$$

where ϵ is the effective energy necessary to produce an electron-hole-pair. For germanium this value is $\epsilon = 2.96$ eV.

The intrinsic energy resolution is dependent on the number of charge carriers. From (3.1), the expected variation of electron-hole-pairs is:

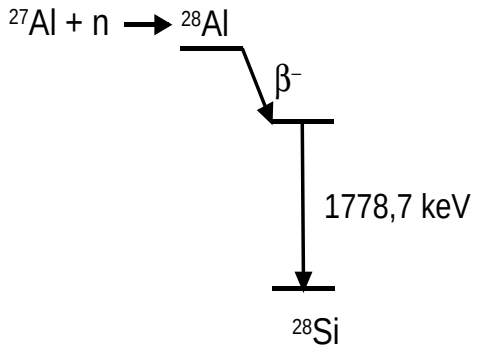

Figure 3.9: Decay scheme of activated Aluminium (compare scheme in the appendix).

$$\sigma_n = \sqrt{n} = \sqrt{\frac{E_\gamma}{\epsilon}}. \tag{3.2}$$

The energy resolution Δ now is given by the full width at half maximum (FWHM) of the photopeak. Δ is assigned to the standard deviation σ according to $\Delta = 2.355 \cdot \sigma$. Assuming the number of electron-hole-pairs produced in the crystal is poisson-distributed, σ is given by:

$$\sigma = \epsilon \cdot \sigma_n = \sqrt{E_\gamma \cdot \epsilon}, \tag{3.3}$$

and Δ:

$$\Delta = 2.355 \cdot \sigma = 2.355 \cdot \sqrt{E_\gamma \cdot \epsilon}. \tag{3.4}$$

For an example: $E_\gamma = 1300$ keV gives a theoretical energy resolution of $\Delta = 4.6$ keV. In reality, the naive assumption of poisson statistics is incorrect. And indeed, it is observed that the resolution of many such detectors is actually smaller than that calculated from poisson statistics. The reason is, because statistically the ionisation events are not all independent so that poisson statistics is not applicable.

So we introduce the Fano-Factor: the Fano-Factor is a ratio that describes the energy resolution of the detector. It is defined as follows:

$$F = \frac{measured\ resolution}{theoretical\ resolution} \ .$$

Typical values are 0.2 and smaller.

Figure (3.10) shows a typical γ-spectrum of activated Aluminium. The only stable isotope ^{27}Al possess an absorption cross section of 0.23 barn for thermal neutrons and gets activated to ^{28}Al by neutron absorption (see figur 3.9). ^{28}Al decays via β^--decay into ^{28}Si with a half life of 2.24 minutes. This decay is not directly into the ground state of ^{28}Si, it populates an exited state, which decays under emission of a 1.779 MeV γ-quantum after 0.5 ps (compare decay scheme of Aluminium in the appendix.).

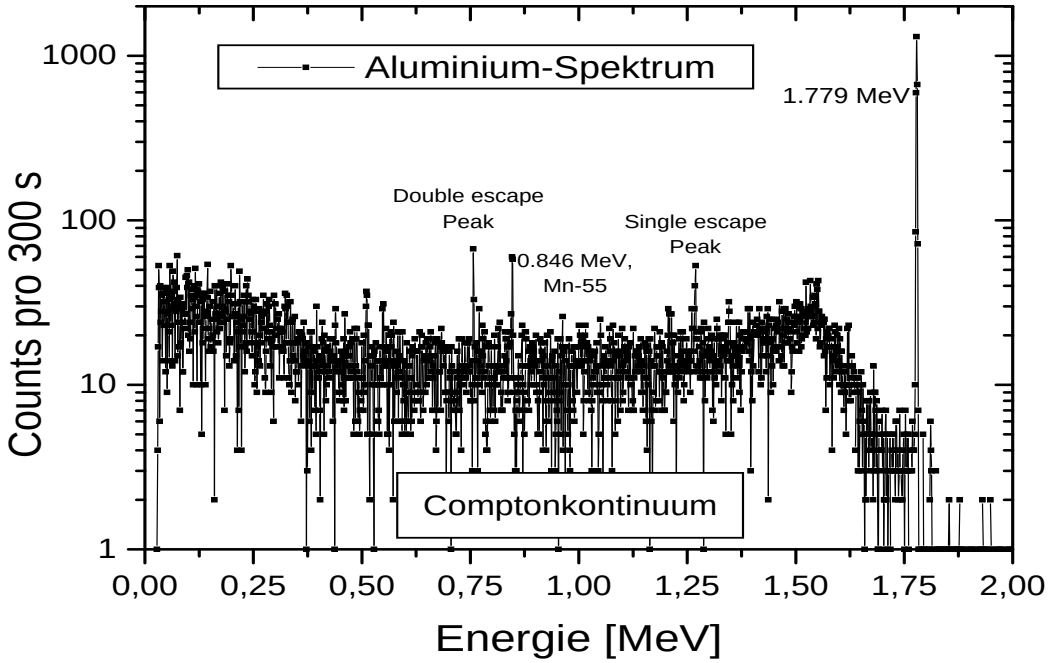

Figure 3.10: γ-spectrum of activated Aluminium. The additional peak at 846 keV comes from a admixture of ^{55}Mn.

3.2 Measurements

In this experiment 11 different probes are available. The neutron source will be used to activate three unknown samples. The energy of the gamma radiation from these activated sources will be recorded by the Germanium-detector and transferred via serial line to the PC. Also the background spectrum should be measured. Every measurement takes 300 s. In the PC, all data have to be recalibrated from PHS channels into energy channels. Then the measured spectra can be compared to theoretical decay schemes in order to identify the sources.

Element	Isotope	Natural Abundance	σ_{abs} [barn]	decays to	Half Time $t_{\frac{1}{2}}$	Final Nucleus
Aluminium	^{27}Al	100%	0.23 barn	^{28}Al	2.24 min	^{28}Si
Barium	^{138}Ba	71.7%	0.35 barn	^{139}Ba	82.9 min	^{139}La
Holmium	^{165}Ho	100%	63 barn	^{166}Ho	26.8 h	^{166}Er
Iodin	^{127}I	100%	6.2 barn	^{128}I	24.99 min	^{128}Xe, ^{128}Te
Copper	^{63}Cu	69.17%	4.5 barn	^{64}Cu	12.7 h	^{64}Ni
	^{65}Cu	30.83%	2.17 barn	^{66}Cu	5.1 min	^{66}Zn
Lanthanum	^{139}La	99.91%	9 barn	^{140}La	40.3 h	^{140}Ce
Manganese	^{55}Mn	100%	13.36 barn	^{56}Mn	2.579 h	^{56}Fe
Neodym	^{148}Ne	5.76%	2.48 barn	^{149}Ne	1.73 h	^{149}Pm
Vanadium	^{51}V	99.75%	4.88 barn	^{52}V	3.76 min	^{52}Cr
Europium	^{151}Eu	47.8%	5900 barn	^{152}Eu	13.5 a/9.3 h	^{152}Sm/^{152}Gd
Tungsten	^{186}W	28.6%	37.8 barn	^{187}W	23.9 h	^{187}Re

Table 3.1: Probes, which are available for the activation analysis. The decay schemes of these probes can be found in the appendix.

The calibration of the PHS is as follows:

$$energy[keV] = 1.1495 \cdot channel + 7.880. \tag{3.5}$$

- **Substract** from every measured probe spectrum the background spectrum!
- Then identify the probes by comparison of the measured spectra to the theoretical decay schemes. For this reason, it is worth to plot the spectra in a logarithmic scale (compare figure 3.10)!
- From one of these energy spectra, the Fano-Factor, a measure of the energy resolution of the detector, has to be calculated.
- For one spectrum, please determine the intensities of the γ-lines and compare the relative intensity of the most prominent decay lines to the theoretical values given in the decay schemes in the appandix. Please notice, that the efficiency of the detector depends on the energy of the γ-ray. So you will have to correct for this your data. The formula for correction is as follows:

$$correction\ factor = 2.26 \cdot energy[MeV] + 0.17. \tag{3.6}$$

Chapter 4

Time of Flight Spectrum

The neutron source used in the experiment delivers prevailingly thermal neutrons, made so by the polyethylene moderator. It is important to recognize that the neutron beam is not a monochromatic one. The velocity of the neutrons vary theoretically according to a Maxwell distribution, described in terms of an average temperature, T_0, that corresponds to the temperature of neutrons that experience complete moderation. The Time of Flight, or TOF, spectrum will now be measured for discrete packets of neutrons, created from the continuous neutron source by a Chopper. The same 3He-detector from the other tasks measures the time for each neutron in the pulse over the path length, s, defined as the distance between the Chopper and the detector (see figure 4.1).

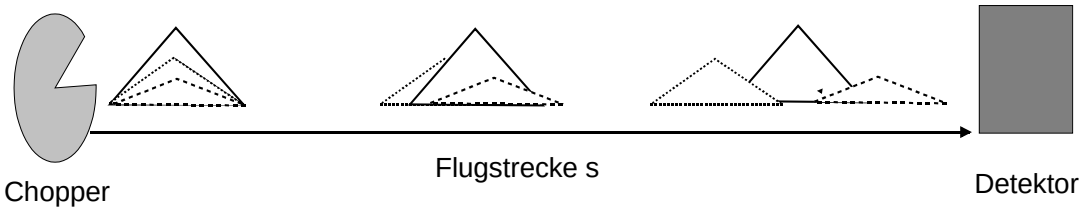

Figure 4.1: Schematic setup of the TOF-measurement to determine the velocity distribution in the neutron beam.

The Chopper consists of a disc made of a material impermeable to neutrons (cadmium), and four "openings," or slits, made of a material transparent to neutrons (aluminium). It rotates with a frequency perpendicular to the direction of radiation from the source. The small size of the slit lets through only a pulse of neutrons, whose different velocities cause them to disperse over the flight path and reach the detector at different times. The detector is connected to a PC-card, so that neutrons that reach the detector at different times are sorted into different time-channels k ($= t \cdot$ dwelltime). The dwelltime, the width of each time-channel, can be set up in the programm at the PC.

4.1 The Chopper

As already mentioned before, the Chopper consists of a disc made of a material impermeable to neutrons (cadmium), and four "openings," or slits, made of a material transparent to neutrons (aluminium) (see figure 4.2). It rotates with a frequency perpendicular to the direction of radiation from the source. The flight path distance and the frequency of the Chopper are optimized to get best results at about s $\approx$ 0.30 cm and $\nu_{Chopper} \approx 200$ Hz.

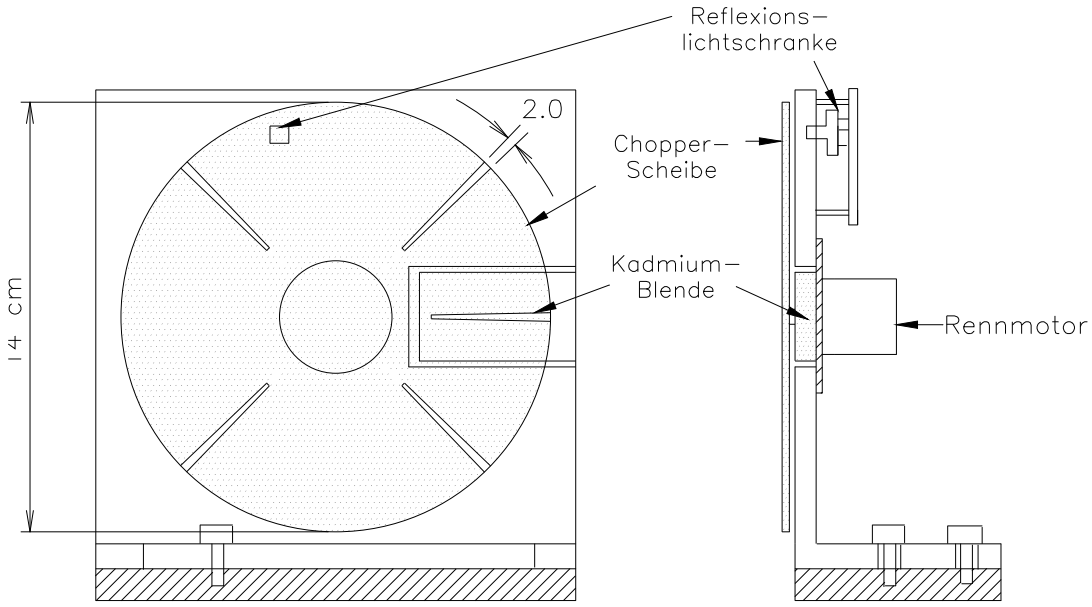

Figure 4.2: Beam chopper for the TOF measurement.

A photo-electric barrier on the Chopper disc determines the start time of the measurement. The detector is connected to a PC-card, so that neutrons that reach the detector at different times are sorted into different channels. The time-width of the channel, or dwell-time, corresponds to a predetermined TOF-interval.

Since the aperture has the shape of an arc length, the opening function O(k) of the chopper is a triangle (see figure 4.3). The opening function O(k) describes which portion of the radiation is let through the Chopper at time t respective time channel k.

$$O(k) = \begin{cases} 0, & k < k_0 - \Delta \\ 1 + \dfrac{k - k_0}{\Delta}, & k_0 - \Delta \leq k < k_0 \\ 1 - \dfrac{k - k_0}{\Delta}, & k_0 \leq k < k_0 + \Delta \\ 0 & k \geq k_0 + \Delta \end{cases} . \tag{4.1}$$

The value k_0 (see equation 4.2) is the number of the first channel at which the Chopper is fully opened, and the neutrons that we wish to detect are allowed through. The counts that we have

in the channels chronologically before this channel are part of the underground spectrum, that we assume is constant and always present.

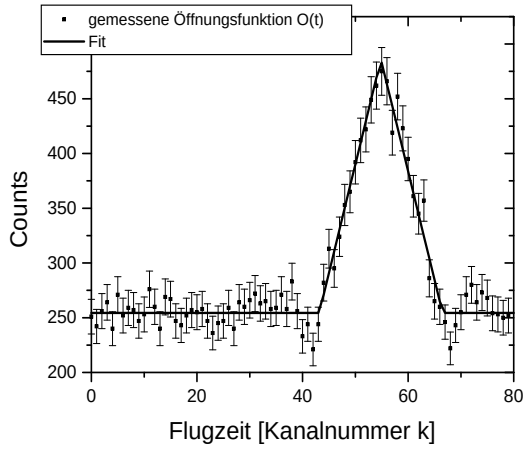

Figure 4.3: Measurement and fit of the opening function O(k) of the chopper disc according to [Th99].

$$k_0 = \frac{43.605}{1401.6 \cdot \nu_{Chopper}[Hz] \cdot dwelltime[s]} \; . \tag{4.2}$$

The dwelltime is the width of each channel in time; this can be changed on the settings in the PC. In our case, the dwelltime should be 2.5 μs. The Chopper frequency $\nu_{Chopper}$ can be determined from the TOF measurement; since the TOF-card begins counting with each new trigger pulse, the last filled channel gives the actual counting period, the inverse of which is the frequency $\nu_{Slit} = 4 \cdot \nu_{Chopper}$.

The width Δ of the triangle function for this chopper is given as:

$$\Delta = \frac{9.78}{1401.6 \cdot \nu_{Chopper}[Hz] \cdot dwelltime[s]} \; . \tag{4.3}$$

4.2 Measurement

The ^{3}He counter tube has to be mounted onto the basic plate of the chopper at the marked position. The length of the flight path s between chopper and detector can be measured with a meter rule. Then, put the setup into the neutron beam. The detector runs as described in chapter (2). Finally, connect the chopper motor and the photo-electric barrier with power supply.

The positive signal form the photo-electric barrier has to be connected via a level converter[1] with the Trigger-input[2] (Trig) of the TOF-card in the PC (see figure 4.4). The Gate-signals of the detector should be connected to the counter input (In1) at the TOF-card.

The program "TOF" controls the TOF-card. The standard values (1024 channels, dwelltime = 2.5 μs) should allow the measurement of a suitable TOF-spectrum. The measurement itself takes about one night to get enough statistics.

[1]The level converter serves here only as an additional current driver, to match the signal of the photo-electric barrier onto the input impedance of the TOF-card.

[2]The Trigger-input needs a positive Trigger-signal.

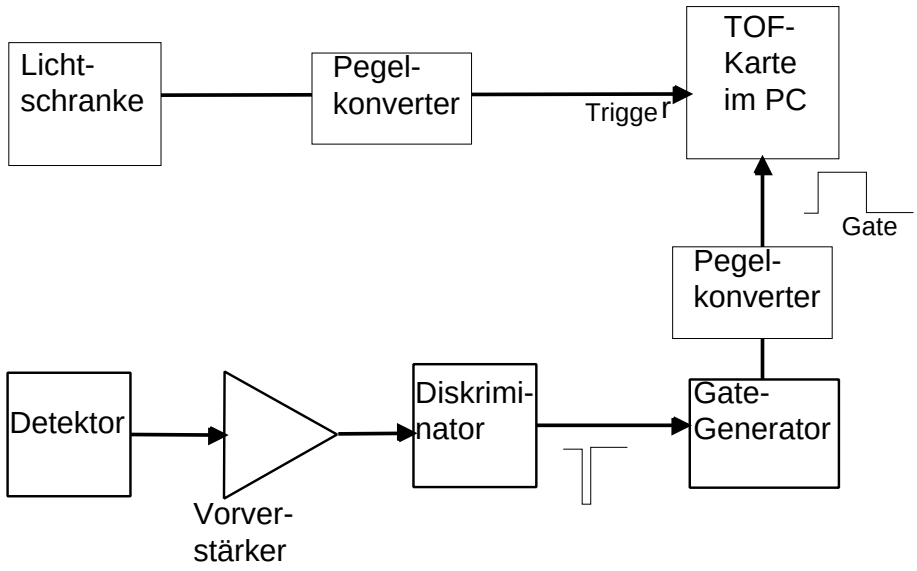

Figure 4.4: Setup of the readout electronic for the TOF measurement.

4.3 Theory

The Maxwell distribution for the velocities of the neutrons inside the source N(v, T) is given by:

$$N(v,T)\ dv = \sqrt{\frac{2}{\pi}}\ \left(\frac{m}{k_B T}\right)^{\frac{3}{2}}\ v^2\ exp(-\frac{mv^2}{2k_B T})\ dv \tag{4.4}$$

so that the neutron beam escaping form the hole in the biological shield of the source will have following velocity distribution S(v, T):

$$S(v,T)\ dv = \frac{1}{2}\ \left(\frac{m}{k_B T}\right)^{2}\ v^3\ exp(-\frac{mv^2}{2k_B T})\ dv, \tag{4.5}$$

with the average velocity $\bar{v}$

$$\bar{v} = \frac{3}{2}\ \sqrt{\frac{\pi k_B T}{2m}}\ . \tag{4.6}$$

This beam spectrum S(v, T) corresponds to the neutron flux density j = n·v = N(v, T)·v, escaping from the source and flying along the flight path s into the detector.

Assuming that the number of neutrons let through by the Chopper is the same each time, the TOF spectrum of the neutrons, D(t, T) can be related to the velocity distribution S(v, T) as follows:

$$\int D(t,T)dt = \int S(v,T)dv\ \Rightarrow\ D(t,T) = S(v,T)\mid \frac{dv}{dt} \mid\ . \tag{4.7}$$

So that the TOF spectrum D(t, T) in dependency of the flight time t is:

$$D(t,T) = \frac{1}{2} \left(\frac{ms^2}{k_B T}\right)^2 t^{-5} \, exp(-\frac{ms^2}{2k_B T t^2}). \tag{4.8}$$

In this equation, the constants are m_n the mass of a single neutron, k_B the Boltzmann constant and s the path length. In terms of time-channels k, the TOF spectrum can be written (again according to transformation (4.7)):

$$F(k,T) = D(t = k * dwelltime, T) \mid \frac{dt}{dk} \mid \tag{4.9}$$

$$F(k,T) = \frac{1}{2} \left(\frac{ms^2}{k_B T}\right)^2 dwelltime^{-6} \, k^{-5} \, exp(-\frac{ms^2}{2k_B T (k * dwelltime)^2}). \tag{4.10}$$

This equation, however, assumes that the incident neutron packet is, as in the ideal case, a delta function. In reality, the neutron packet has a finite width already at the start, the form of which depends upon the construction of the Chopper (compare figures 4.2 and 4.3).

The opening function O(k) describes which portion of the radiation is let through the Chopper at time-channel k. So the measured TOF spectrum M(k′, T) is in reality a convolution of the opening function O(k) with the TOF spectrum F(k, T):

$$M(k') = \int_{-\infty}^{+\infty} F(k,T) \cdot O(k' - k) \, dk \tag{4.11}$$

In this experiment the broadening of the TOF spectrum according to the opening function will be ignored. The measured data will be directly compared to F(k, T) (equation 4.10).

4.4 Calculation

Goal of the calculation is to determine the mean temperature T_0 of the moderated neutron spectrum according to equation (4.10). To find the temperature, we vary the parameter T of the theoretic spectrum F(k, T) in equation (4.10) until the best agreement between data and theory is found.

First, we generate a theoretical spectrum, F(k, T) (k = 1, ..., 1024), where k is the channel number. To compare theory quickly to experimental data (TOF_k) and to optimize this fit, it is useful to write a small computer program.

The program calculates the so-called χ^2 for every possible theory onto the data. This statistical comparison, we make, compares the average square of the deviation of the theory to the measured data. The deviation between theory and experiment is calculated for each channel and normalized with the uncertainty of the measurement.

$$\left(\frac{TOF_k - F(k,T)}{\Delta TOF_k}\right)^2 \tag{4.12}$$

The sum of all the deviations is a measurement of how strongly the measured data spreads in reference to the theory. The χ^2 is defined as follow that a χ^2 equal to "N" means, that in the statistical limit all data are in agreement with theory.

$$\chi^2(T) = \sum_{k=1}^{N} \left(\frac{TOF_k - F(k,T)}{\Delta TOF_k} \right)^2 . \tag{4.13}$$

The program to be written should increment the temperature in a certain range in some steps (e.g. from 200 K to 400 K, by increments of 5 K) and calculates the corresponding χ^2. When plotted as χ^2 versus T, it forms a distribution with a minimum, the optimum value for T_0 (see figure 4.5). Since χ^2 is defined in units of standard deviation, the uncertainty ΔT in the mean temperature can also be read from the graph.

To the data collected, certain corrections must be made before the values can be compared to theory:

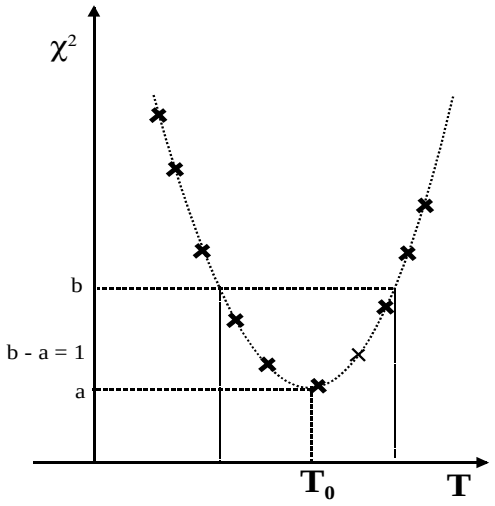

Figure 4.5: Determination of the mean temperature T_0 of the neutron spectrum with the aid of the χ^2-method.

First, there is an offset in the TOF spectrum due to the mechanical setup of the Chopper; the offset corresponds to the time difference between when the light window delivers a start signal and when the neutrons begin to fly. This is determined by the k_0 value from equation (4.2). Second, the background spectrum must be determined and subtracted. This can be done by averaging the values over a portion of the graph in which we are sure that there are no thermal neutrons (at high channel numbers) and subtracting from the total. Finally, the counts must be normalized. To do this, we integrate over the entire spectrum (without the background, starting from k_0) to determine the total number of counts, and divide the number in each channel by the total number to normalize to unity.

- Please attach to your report the listing of your small program or a comparable print, so that one can understand what you have done.
- Furthermore, a plot of the χ^2 distribution is needed, in which the values of T_0 and ΔT can be seen!
- Then a plot of the fitted TOF spectrum, this means a plot where the corrected data TOF_k and the theoretic curve F(k, T_0) of the determined temperature are shown together.
- Finally, a plot of the velocity distribution S(v, T_0) of the neutron beam.

Chapter 5

Radiography

Radiography with X-rays is a well known technique in medicine or material science. What about neutrons? They have no charge, and their electric dipole moment is either zero or too small to be measured by the most sensitive of modern techniques. For these reasons, neutrons can penetrate matter far better than charged particles or photons. Furthermore, neutrons interact with atoms via nuclear rather than electrical forces, and nuclear forces are very short range - of the order of a few fermis (1 fermi = 10^{-15} m). Thus, as far as the neutron is concerned, solid matter is not very dense because the size of a scattering center (nucleus) is typically 100000 times smaller than the distance between such centers. As a consequence, neutrons can travel large distances through most materials without being scattered or absorbed. The attenuation, or decrease in intensity, of a beam of low-energy neutrons by aluminum, for example, is about 1% per millimeter compared with 99% or more per millimeter for X-rays. Figure (5.1) demonstrates this point for X-rays and neutrons.

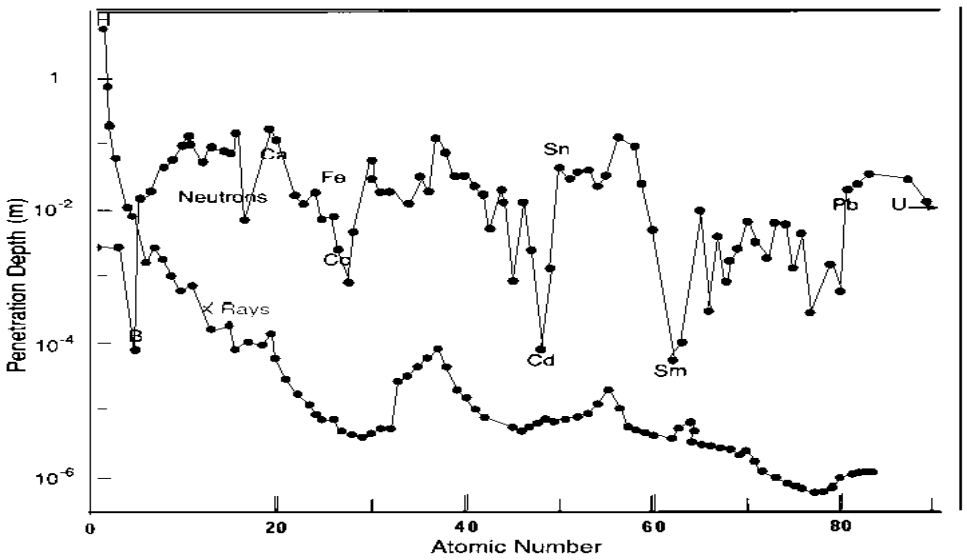

Figure 5.1: Depth of penetration for neutrons and X-rays in comparison [LA90].

To make radiography with neutrons, it is necessary to have a camera for neutrons. For this, neutrons have to be converted via nuclear reaction into charged particles similar to the ^{3}He counter tube. The energetic charged particles then are able to make black a film layer.

There exist several nuclear reactions with a sufficient high absorption cross section for thermal neutrons to produce suitable charged particles:

$$n + {}^{10}B \longrightarrow \alpha + {}^{7}Li,\ \sigma = 3835\ barn$$

$$n + {}^{6}Li \longrightarrow {}^{3}H + {}^{4}He,\ \sigma = 940\ barn$$

$$n + {}^{157}Gd \longrightarrow {}^{158}Gd + e^- + \gamma,\ \sigma = 259000\ barn$$

Furthermore, we need an amplifier for the signals of these nuclear reactions because of the very low flux of our Californium source. We solve this problem by using a scintillator.

To get an optimal resolution we use a commercial scintillator specialized for neutron detection. The scintillator consists of ^{6}Li to convert neutrons into charged particles (α-particle and tritium). Both of these products of the nuclear reaction interact with the ZnS(Ag) of the scintillator and so they produce light in the scintillator (about 10^5 photons per neutron). The ^{6}LiF is a fine powder mixed with the ZnS(Ag) as a fine powder as well. Both are glued onto 1 mm thick Aluminium sheet. Such a neutron detector will be placed in front of a film of an ordinary polaroid camera to make pictures with neutrons.

5.1 Measurement

Make several radiographies of different materials. Think about which combination of materials will give a good contrast onto the film.

Bibliography

[By94] J. Byrne; Neutrons, Nuclei and Matter; Bristol: Institut of Physics Publishing

[Ca98] C. Caso et al, The European Physical Journal, C3 (1998) 1

[ILL00] ILL, Millenium Programm, "Exploring matter with neutrons, Highlights in research at the ILL", (2000), http://www.ill.fr/pages/science/AtILL/brochures.html

[Kr88] Kennth S. Krane, Introductory nuclear physics, John Wiley & Sons, New York 1988

[LA90] Los Alamos Science: http//lib-www.lanl.gov/la-science/n19/index.html

[Le78] C.M. Lederer, V.S. Shirley; Table of Isotopes; New York/Chichester/Brisbane/Toronto: Wiley & Sons (1978)

[Ma98] I. Mauch; Aufbau eines Praktikumsversuches und neutronenphysikalische Experimente; Staatsexamensarbeit Univ. Heidelberg (1998)

[Mi] A. Michaudon, S. Cierjacks, R. E. Chrien: *Neutron Sources For Basic Physics and Applications*, Neutron Physics and Nuclear Data in Science and Technology, Vol. 2

[Re] Reuter-Stokes Betriebsanleitung; Fundamentals of Helium-3 Filled Proportional Counters for Neutron Detection; Twinsburg, Ohio

[Th99] N. Thake; Experimente zur Neutronenphysik im Fortgeschrittenenpraktikum; Staatsexamensarbeit Univ. Heidelberg (1999)

[Su76] G. Subrahmanian, G. Venkattaraman, U. Madhvanath: *Radiatiation Protection Aspects in the Use of Californium-252 Sources* in *Some Physical, Dosimetry and Biomedical Aspects of Californium-252*, International Atomic Energy Agency, Wien (1976)

[Ye97] The Yellow Book; Guide to Neutron Research Facilities at the ILL, December 1997, http://www.ill.fr/pages/science/IGroups/sc_frst_2.html

Appendix A

Decay Schemes

The following decay schemes are from the book "Table of Isotopes" [Le78]. On the upper left corner, you will find the mother nucleus (atomic mass number, half life time, etc.) and, in the middle at the bottom of the scheme, the daughter nucleus. The numbers in percentage at the left side are the branching ratios the levels of the daughter nucleus are populated by a decay of the mother nucleus. Furthermore, for every γ-line its relative appearance in the hole spectrum is given as well as the energy of the emitted γ-photon (bold number) in terms of keV.

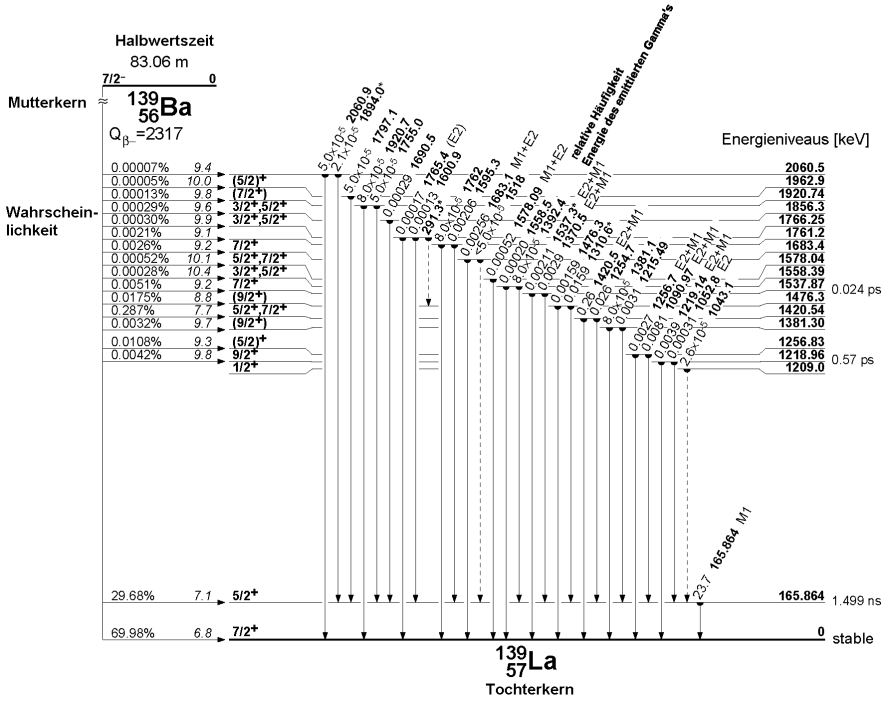

Figure A.1: Decay scheme of activated Barium

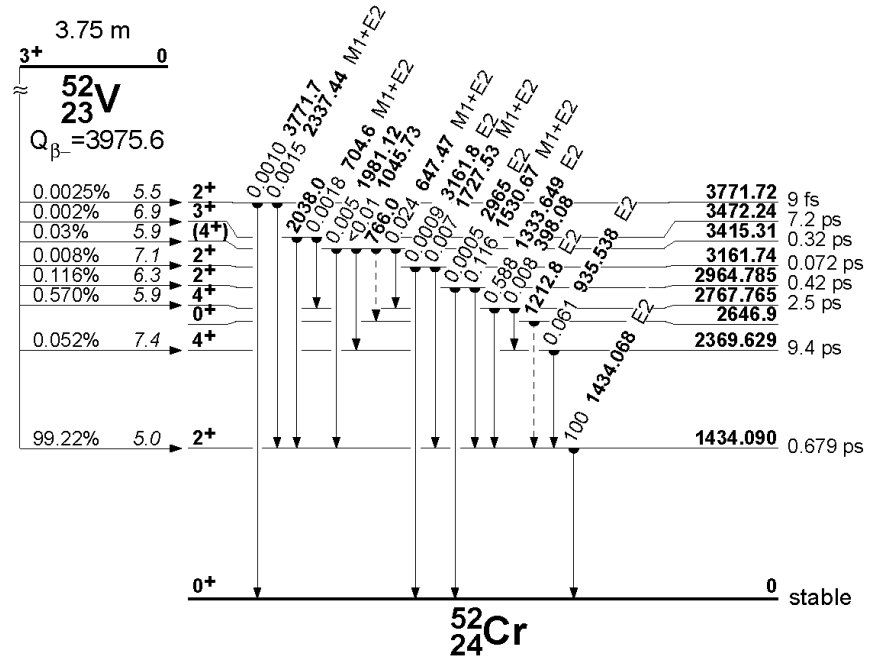

Figure A.2: Decay scheme of activated Vanadium

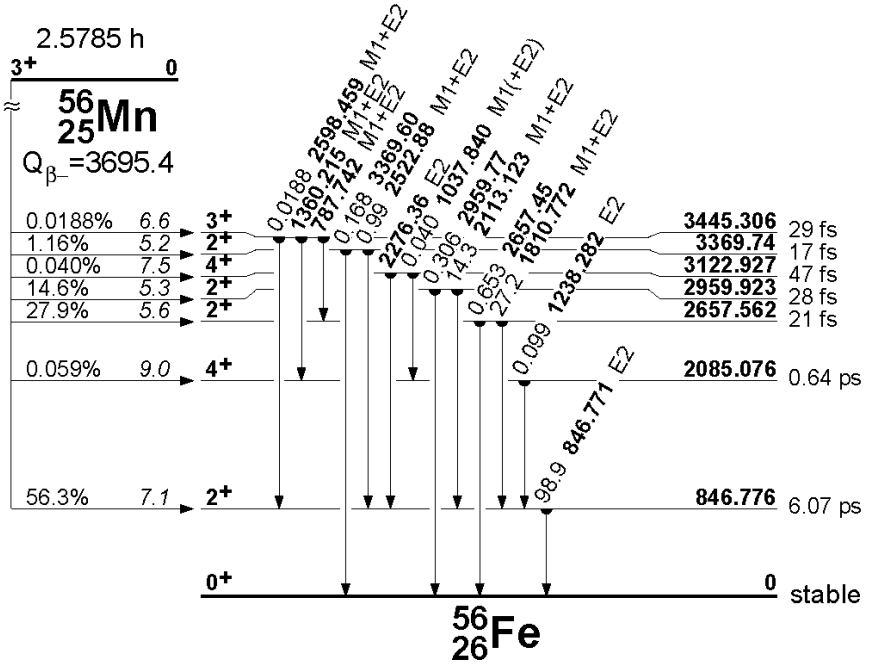

Figure A.3: Decay scheme of activated Manganese

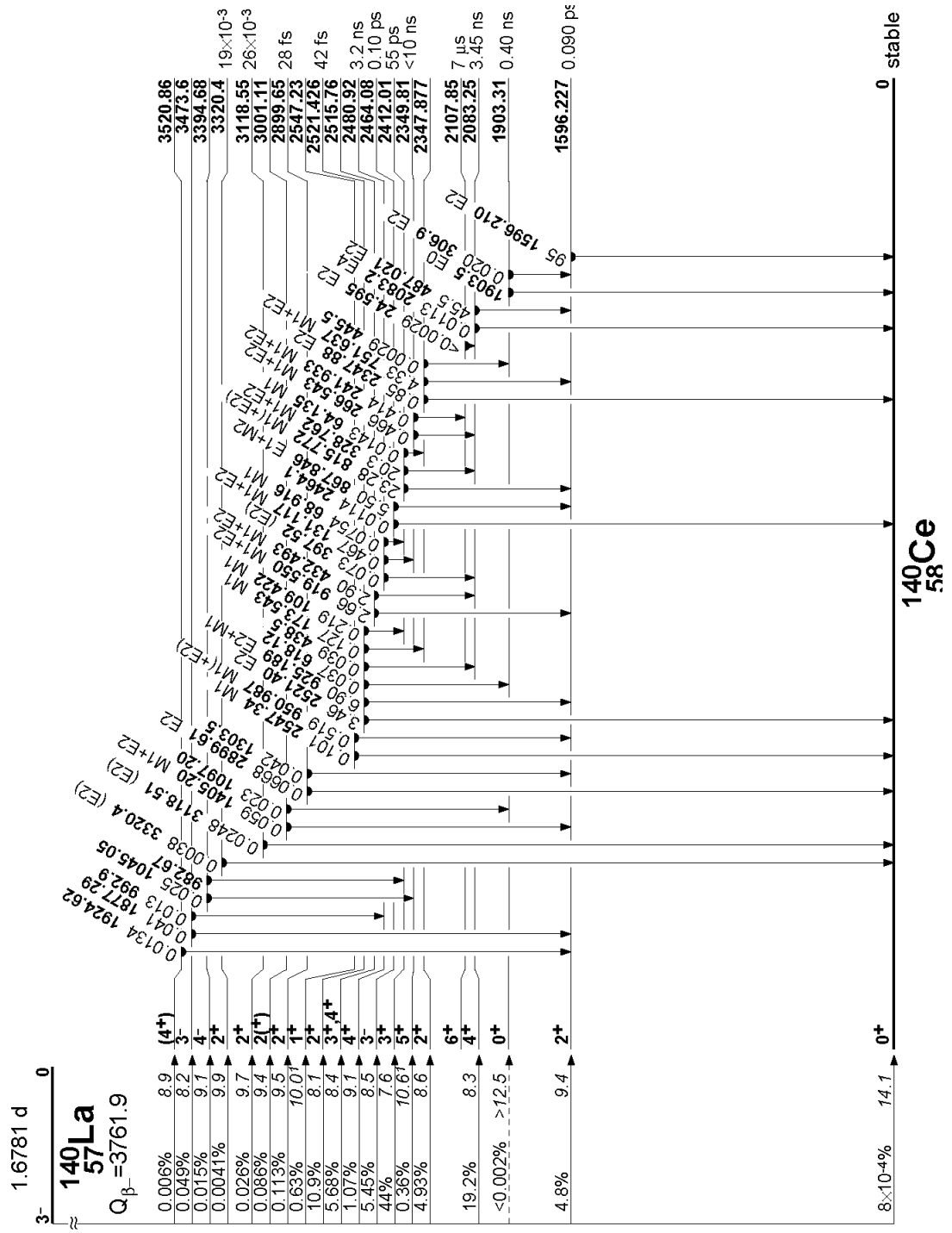

Figure A.4: Decay scheme of activated Lanthanum

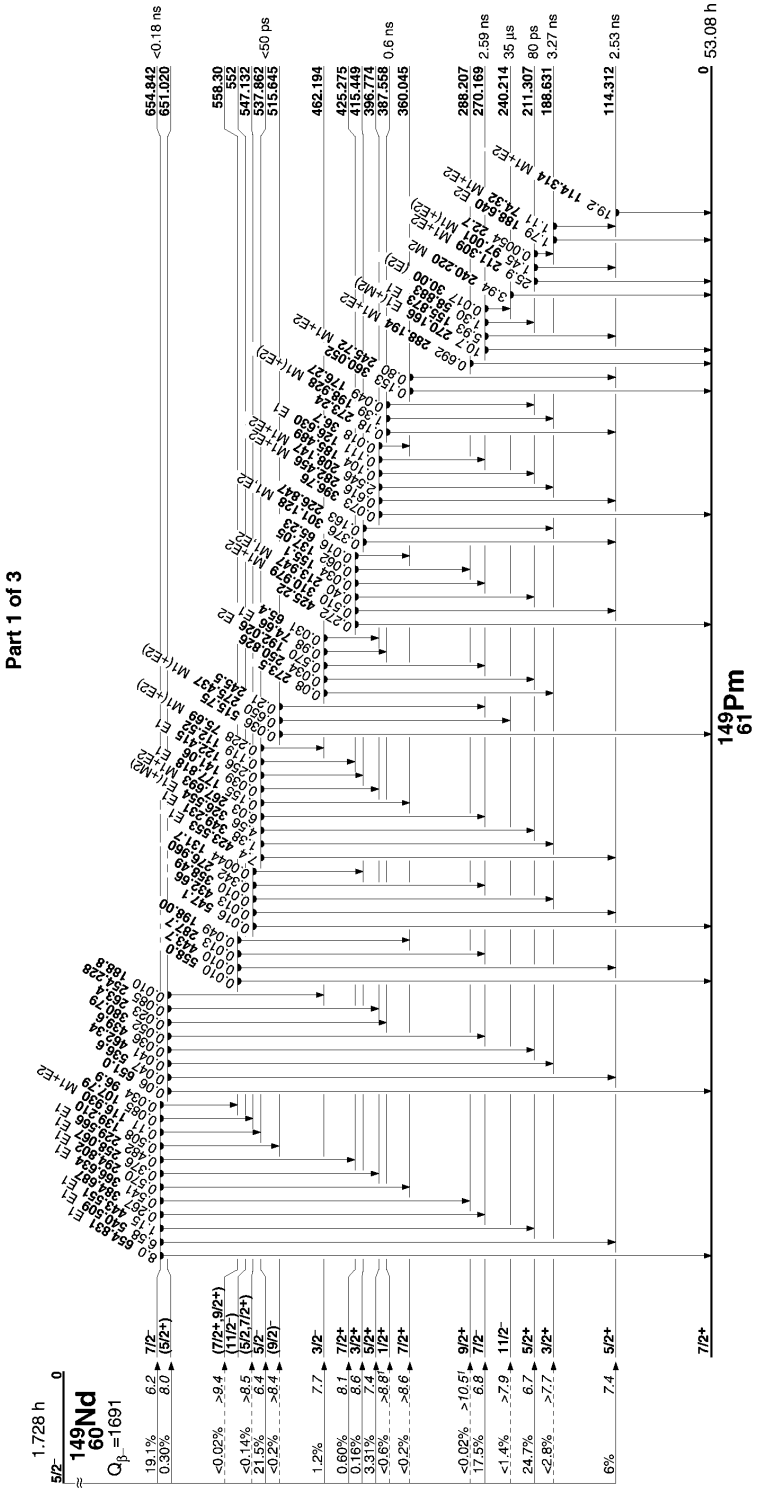

Figure A.5: Decay scheme of activated Neodym

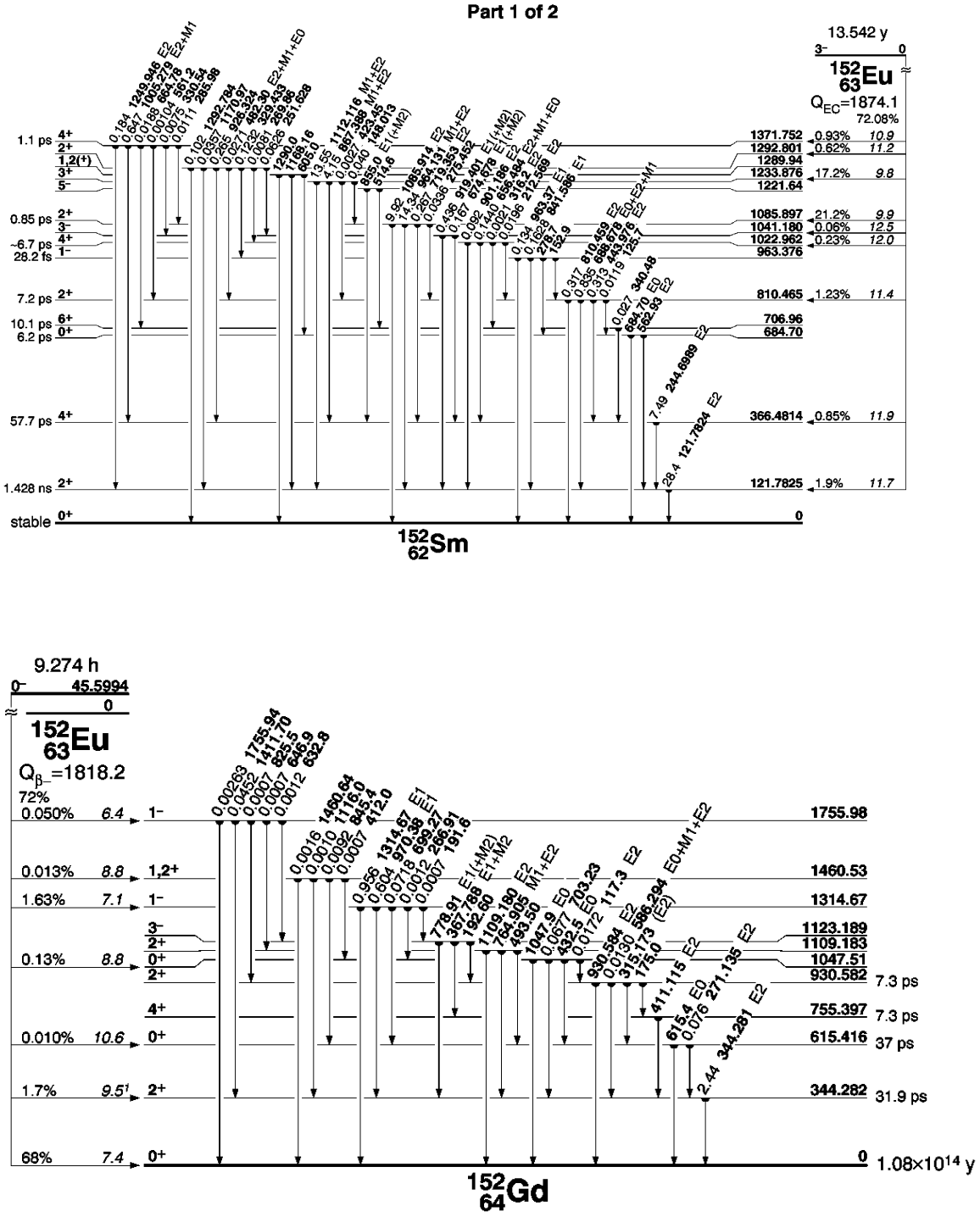

Figure A.6: Decay scheme of activated Europium

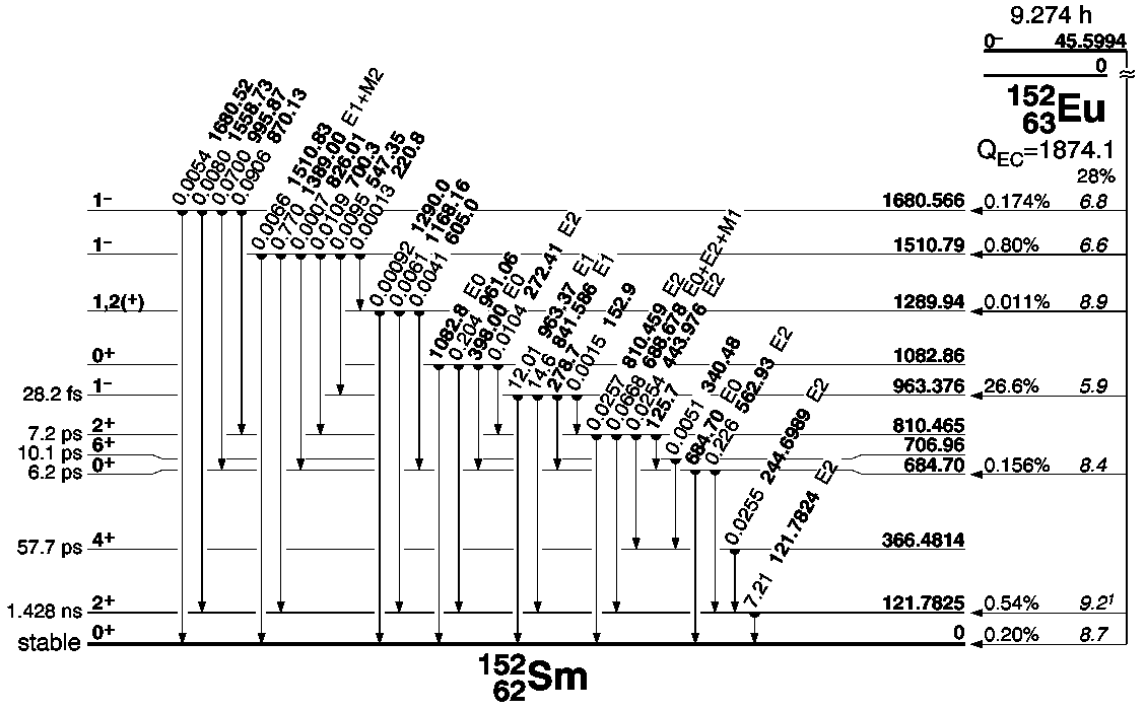

Figure A.7: Decay scheme of activated Europium

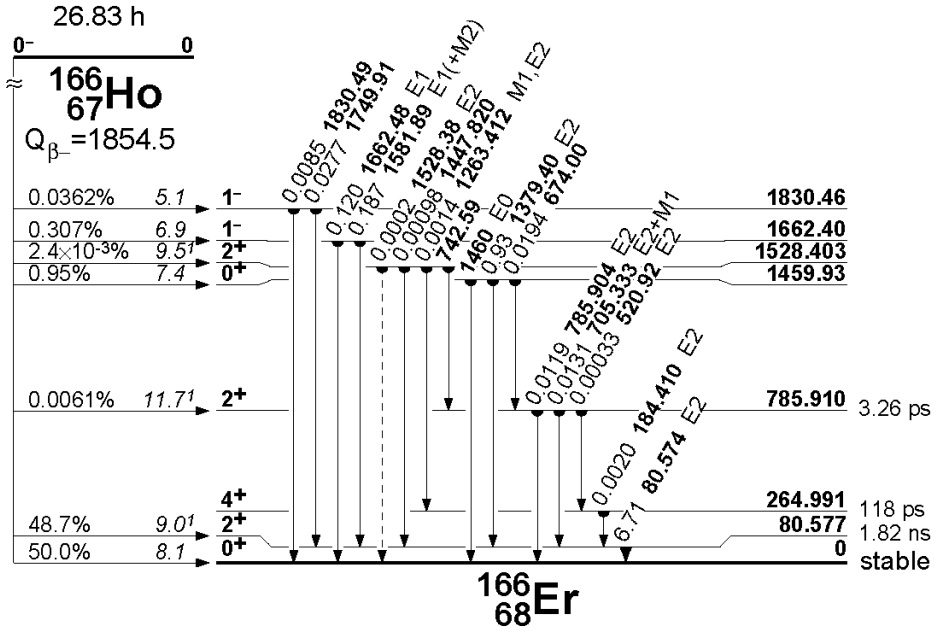

Figure A.8: Decay scheme of activated Holmium

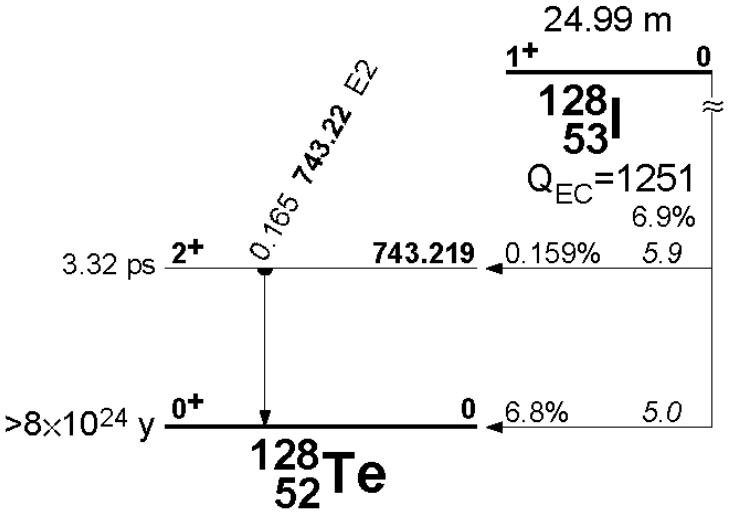

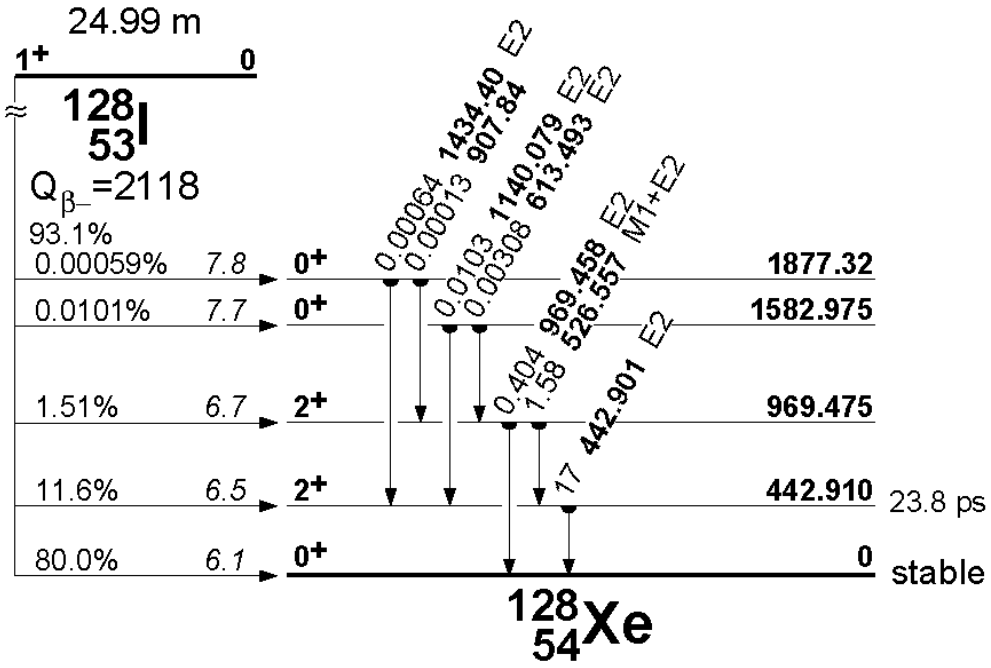

Figure A.9: Decay scheme of activated Iodin

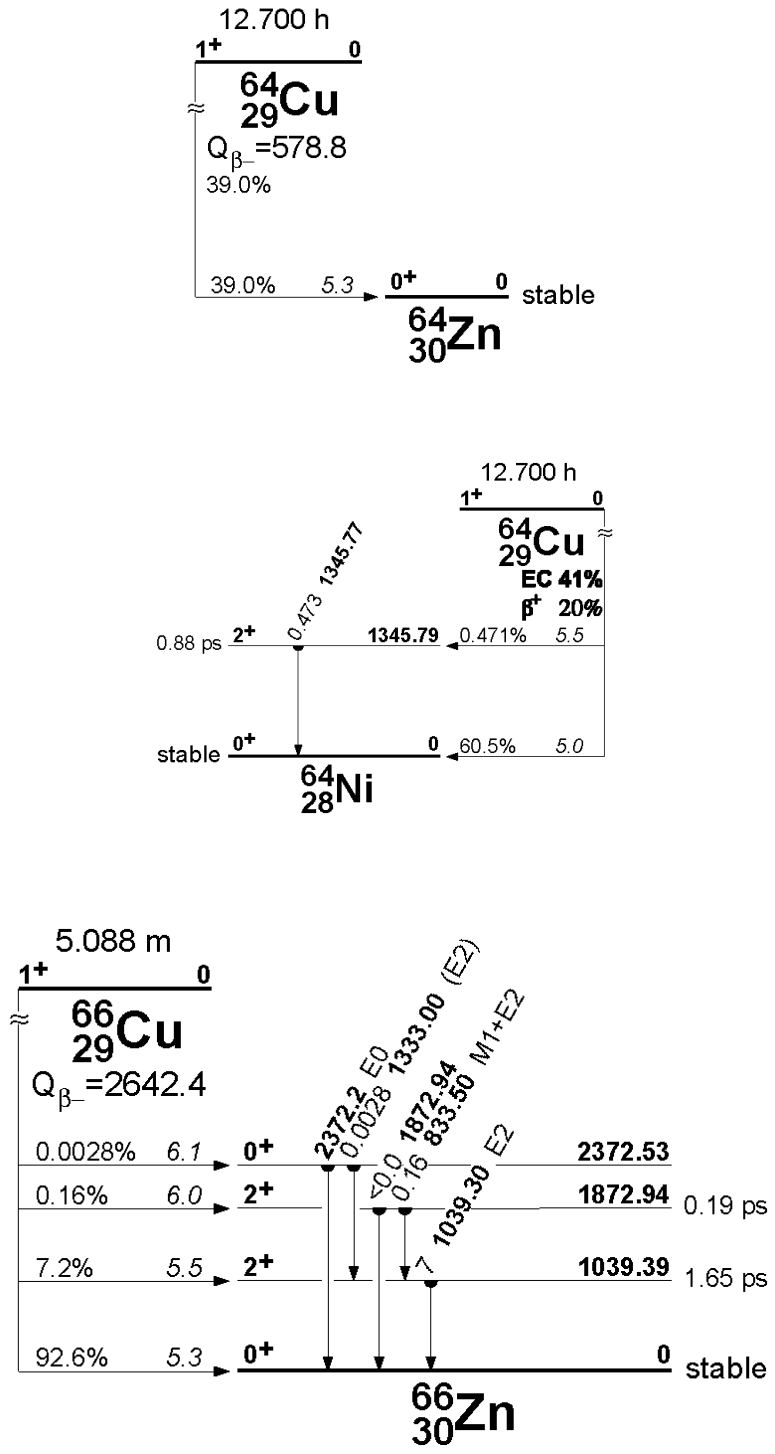

Figure A.10: Decay scheme of activated Copper

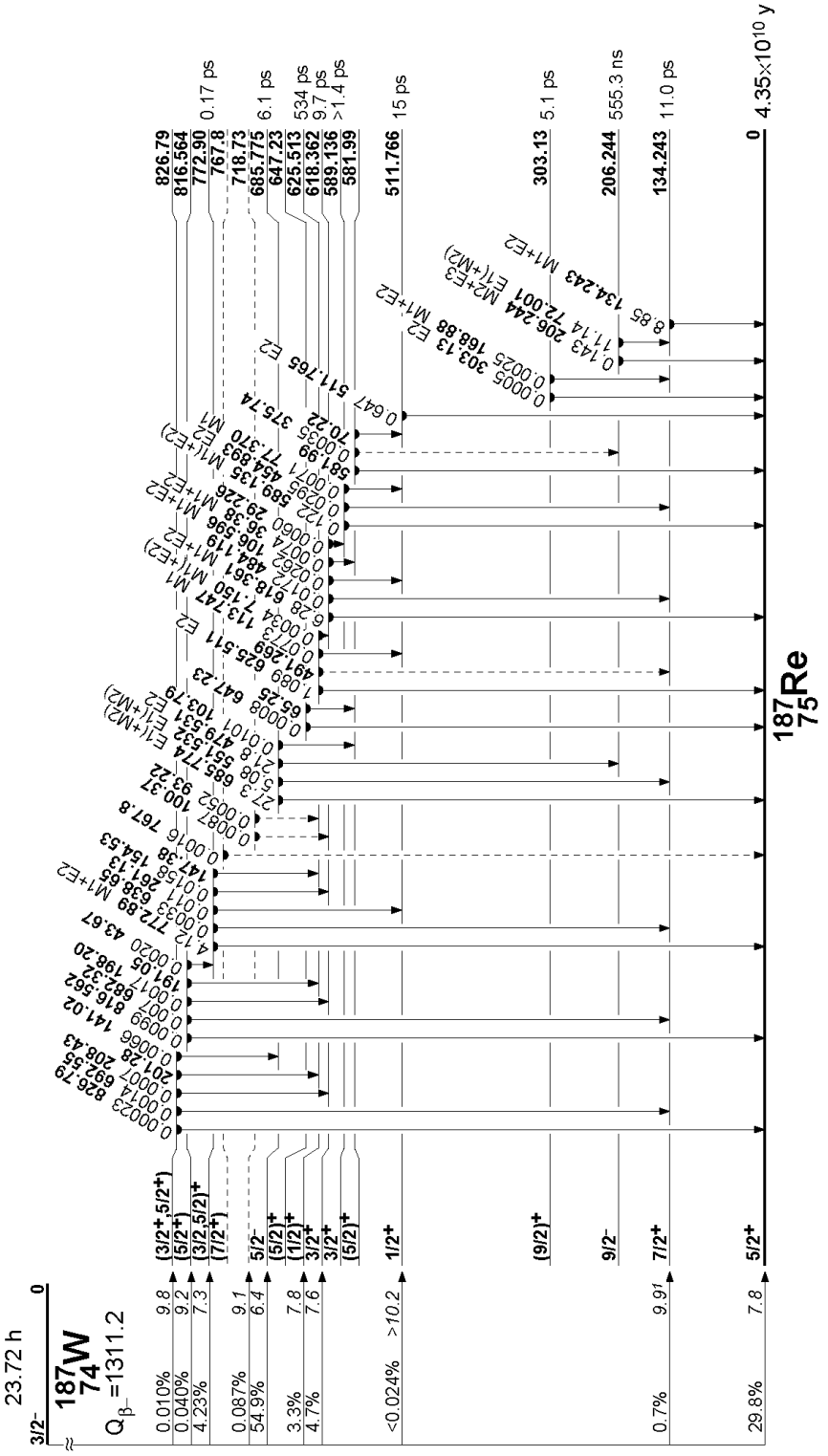

Figure A.11: Decay scheme of activated Tungsten

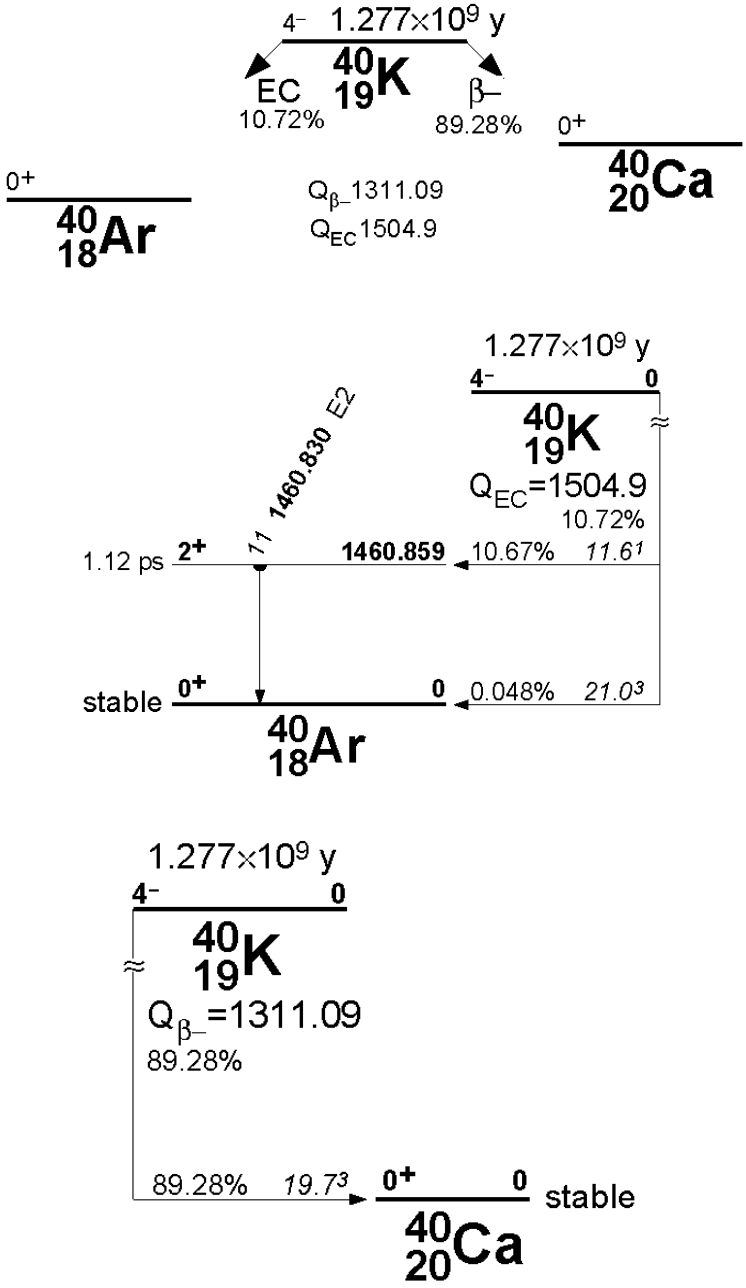

Figure A.12: Decay scheme of activated Potassium

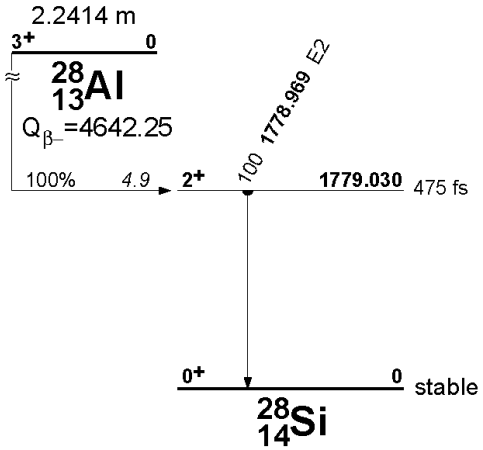

Figure A.13: Decay scheme of activated Aluminium

Appendix B

Questions on F17

B.1 The Neutron

- What are 'thermal neutrons' ?
- What is 'moderation' and what happens on the microscopic scale?
- What's the function of polyethylen and lead as part of the neutron source? Due to which pysical properties are they chosen?

B.2 Neutron Detection

- How does a gas detector work?
- What is a 'pulse height spectrum'? What is shown there?
- How is kinetic energy distributed in a two body decay? How does a three body decay differ?
- What are the reasons for the edge effects of the ^{3}He counter tube?
- What's the use of a 'discriminator' ?

B.3 Activation Analysis

- What is the 'depletion zone' of a n-p-junction? Which physical properties have an influence on its spatial dimensions?
- Which area of semiconductor detectors is sensitive to ionising radiation? How can this region be enlarged?
- What are photo effect, compton effect and pair production?
- How does the 'pulse height spectrum' of a monoenergetic gamma source look like if detected by a semiconductor detector?

- What does the energy resolution of semiconductor detector depend on? How does it compare to the energy resolution of gaseous detectors?
- What's the intensity of a measured gamma line?

B.4 Time of Flight Measurement

- What's the 'velocity distribution' of the neutrons from our neutron source?
- What properties do (density) distribution functions have?
- What is described by the opening function of the chopper?
- What is shown in a time of flight diagram?

B.5 Radiography

- Can neutrons blacken a photographic film?
- Which matrials yield high contrast using X-ray radiography, which using neutrons?

Appendix C

Links to interesting pages on neutron physics:

- http://www.neutron-eu.net/en/index.php: European internet portal for neutron and muon-physics
- http://www.neutronenforschung.de/: german portal for neutron physics
- http://www.frm2.tu-muenchen.de/: the new research reactor in Munich, Germany: the world's most modern neutron source
- http://www.ill.fr: the ILL, the world's most intense neutron source
- http://www.isis.rl.ac.uk/: the english spallation neutron source
- http://www.sns.gov/: SNS, soon the most intense spallation neutron source
- http://www.kfa-juelich.de/ess/: the planned European Spallation Source (ESS)
- http://www.isf.unian.it/isf/links/neutron_sites.htm: links to further pages related to neutrons